Journal of Nuclear Materials 517 (2019) 268–285

Contents lists available at ScienceDirect

Journal of Nuclear Materials

journal homepage: www.elsevier.com/locate/jnucmat

# Early studies on Cr-Coated Zircaloy-4 as enhanced accident tolerant nuclear fuel claddings for light water reactors

Jean-Christophe Brachet [a, *], Isabel Idarraga-Trujillo [a, 1], Marion Le Flem [a, 2], Matthieu Le Saux [a, 3], Valérie Vandenberghe [a, f], Stephane Urvoy [a], Elodie Rouesne [a], Thomas Guilbert [a], Caroline Toffolon-Masclet [a], Marc Tupin [b], Christian Phalippou [c], Fernando Lomello [d], Frédéric Schuster [e], Alain Billard [f], Gihan Velisa [f, 4], Cédric Ducros [g], Frédéric Sanchette [g, h]

[a] CEA, DEN, Service de Recherches Métallurgiques Appliquées (SRMA), Université Paris-Saclay, F-91191, Gif-sur-Yvette, France
[b] CEA, DEN, Service d'Etude des Matériaux Irradiés (SEMI), Université Paris-Saclay, F-91191, Gif-sur-Yvette, France
[c] CEA, DEN, Service d'Etudes Mécaniques et Thermiques (SEMT), Université Paris-Saclay, F-91191, Gif-sur-Yvette, France
[d] CEA, DEN, Service d'Etudes Analytiques et de Réactivité des Surfaces (SEARS), Université Paris-Saclay, F-91191, Gif-sur-Yvette, France
[e] CEA, DEN, Université Paris-Saclay, F-91191, Gif-sur-Yvette, France
[f] IRTES – LERMPS UTBM, 2 place Tharradin, F-25000, Montbéliard, France
[g] CEA, LITEN, DTNM, LCH, Univ. Grenoble Alpes, F-38000, Grenoble, France
[h] Nogent International Center for CVD Innovation, LRC CEA-ICD-LASMIS, UTT, Antenne de Nogent, Pôle Technologique de Haute-Champagne, 52800, Nogent, France

## HIGHLIGHTS

- Coated zirconium-based alloys are studied as enhanced accident tolerant nuclear fuel claddings for light water reactors.
- Several types of PVD coatings, including ceramic nitride and metallic multi-layered materials, are studied.
- Chromium coatings are chosen and further developed.
- Encouraging results, showing improved behavior both in normal operating and upon DBA-LOCA and slightly beyond conditions.

## ARTICLE INFO

*Article history:*
Received 3 December 2018
Received in revised form
1 February 2019
Accepted 14 February 2019
Available online 21 February 2019

*Keywords:*
Enhanced accident tolerant fuel claddings
Coatings
Zircaloy-4
Corrosion
High temperature oxidation

## ABSTRACT

Coatings with thicknesses between a few microns and ~10 μm deposited on a Zircaloy-4 substrate have been studied with the objective to provide a significant reduction in the oxidation-induced embrittlement of the nuclear fuel cladding, especially in accidental conditions, such as LOss-of-Coolant-Accident (LOCA) conditions. This paper deals with the early studies carried out at CEA, several years before the Fukushima-Daiishi events, on different types of coatings obtained by a physical vapor deposition process. The studied coatings included ceramic, nitride and metallic multi-layered ones. The results of this screening analysis showed that the first generation of chromium-based coatings exhibited the most promising behavior: good compromise between oxidation resistance and adhesion to the metallic substrate, good fretting resistance and improved resistance to oxidation in steam at high temperature (Design Basis Accident LOCA conditions and slightly beyond).



## 1. Introduction

Following the Fukushima-Daiichi accident in 2011, increasing international Research and Development (R&D) efforts are focusing on the development of Enhanced Accident Tolerant Fuels (E-ATF) cladding materials for Light Water Reactors (LWRs). Beyond the reference Zr-based claddings currently used, these

* Corresponding author.
*E-mail address:* jean-christophe.brachet@cea.fr (J.-C. Brachet).
[1] now at EDF-R&D.
[2] now at CEA, DEN, Service de la Corrosion et du Comportement des Matériaux dans leur Environnement (SCCME), Université Paris-Saclay, F-91191, Gif-sur-Yvette, France.
[3] now at ENSTA Bretagne, UMR CNRS 6027, IRDL, F-29200, Brest, France.
[4] now at Oak Ridge National Laboratory, Oak Ridge, TN, 37831, US.

https://doi.org/10.1016/j.jnucmat.2019.02.018
0022-3115/

developments include alternative cladding materials such as highly oxidation-resistant FeCrAl ferritic steels, refractory based (Mo) materials and ceramic (SiC/SiC …). Ceramic materials are considered to be a powerful but long-term R&D E-ATF concept [1–10].

Among the E-ATF concepts studied worldwide, coated Zr-based materials appear to be one promising short-term E-ATF cladding concept. Indeed, this concept benefits from several decades of experience and operation of Zr-based fuel cladding in LWRs. Furthermore, as far as it is not too thick, the coating has a limited impact on the clad neutronic properties. Since the Fukushima events, several types of coatings have been studied, including metallic and ceramic coatings, deposited by using several processes (physical vapor deposition, vacuum-Arc, cold-spray, 3D laser coating, …) [11–51]. An overview focusing on their behavior upon normal in-reactor operating conditions and High Temperature (HT) oxidation was recently made in Ref. [35].

At CEA, the very early studies on coated zirconium alloys, including chromium-based coatings, were initiated in the 1960s. But, at that time, the main objective was to enhance the corrosion resistance of zirconium-based alloys exposed to $CO_2$ oxidizing environment for graphite-gas reactor application and not upon HT hypothetical Design Basis Accident (DBA) LOss-of-Coolant Accident (LOCA) conditions for LWRs application. Thus, the corrosion experiments were limited to temperatures lower than 650 °C [52,53]. More recently, but several years before the Fukushima-Daiichi accident, it was decided to evaluate more in depth the capacity of modern Physical Vapor Deposition (PVD) processes to generate coated zirconium alloys with higher resistance to HT steam oxidation in LOCA conditions, in addition to enhanced corrosion behavior under in-service operation conditions. Thus, several types of coatings including ceramic and metallic (multilayered or not) coatings have been studied and tested both upon nominal and HT LOCA conditions. As discussed in this paper, PVD chromium coatings have been chosen from these first-step screening tests. The more recent Framatome-CEA-EDF Cr coatings developments are outside the scope of the present paper and have been published elsewhere [54,63].

## 2. Materials and experimental procedures

### 2.1. Materials

The preliminary coatings considered here have been deposited by a PVD Direct-Current Magnetron-Sputtering (DC-MS) process on low-tin stress-relieved Zircaloy-4. Most of these early studies were carried out on 1.2 mm-thick sheet samples. More recently, coatings were deposited by using a hybrid Direct-Current/High Power Impulse Magnetron Sputtering (DC/HiPIMS) PVD process on cladding tube samples, with an outer diameter and a thickness of 9.5 and 0.57 mm, respectively.

Table 1 gives an overview of the different types of coatings preliminarily studied. Both monolayer and multilayers coatings have been fabricated. The overall coating thickness ranged from 1 to 7 μm while the thickness of the sublayers ranged from ~10 to hundreds of nanometers. The coating materials may be classified into two main families:

- metallic materials, such as NbV, NbCrTi, Cr, NbCrTi and multi-layered Cr/NbCrTi,
- ceramic materials, such as TiN, CrN, and multilayered TiN or CrN/AlTiN.

### 2.2. As-received coating characterizations

Properties of PVD coatings and quality of the coating/substrate bonding strongly rely on the coating material and the deposition process/parameters used, which may induce specific microstructures [65,66]. Thus, before performing corrosion and mechanical tests, homogeneity, grain size and morphology, crystallographic texture and residual/internal stresses of the coating have been characterized in the as-received conditions. For that purpose, multiscale examinations from optical microscopy down to the atomic scale using High Resolution Transmission Electron Microscopy (HRTEM) were performed [67,68]. Additionally, Electron Back-Scatter Diffraction (EBSD) and X-Ray Diffraction (XRD) were used to get more insights into the overall and local crystallographic

**Table 1**
The different types of coatings studied.

| Coating type | Notation | Architecture/period (λ[a]) | Total number of sublayers | Total coating thickness ±0.2 μm |
|---|---|---|---|---|
| TiN | TiN | Single-layered | / | 2.6 |
| CrN | CrN | Single-layered | / | 3 |
| TiN and AlTiN | TiN/AlTiN | Multilayered, λ = 2 × 8 nm | >200 | 3.4 |
| CrN and AlTiN | CrN/AlTiN | Multilayered, λ = 2 × 8 nm | >200 | 3.2 |
| $Nb_{82\%}V_{18\%}$ (at%) | NbV | Single-layered | / | 5 |
| $Nb_{67\%}Cr_{10\%}Ti_{23\%}$ (at%) | NbCrTi | Single-layered | / | 4 |
| Cr | Cr | Single-layered | / | 1 and 5 |
| | Cr/Cr | Multipass, λ = 500 nm | 14 | 7 |
| Cr and $Nb_{67\%}Cr_{10\%}Ti_{23\%}$ (at%) | Cr/NbCrTi M10 | Multi-layered, λ = 2 × 5 nm | >500 | 6 |
| 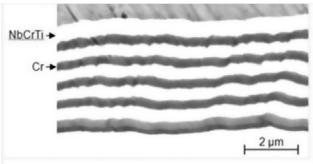  | Cr/NbCrTi M100 | Multi-layered, λ = 2 x (50–80) nm | 40 | 5.5 |
| | Cr/NbCrTi M600 | Multi-layered, λ = 2 × 300 nm | 10 | 6 |
| | Cr/NbCrTi M800 | Multi-layered, λ = 2 × 400 nm | 5 | 4 |

[a] The period corresponds to the number of "layers", i.e. one layer of Cr in the case of Cr/Cr coating and two successive layers of various materials for TiN/AlTiN, CrN/AlCrN and Cr/NbCrTi coatings.

texture of the coating. Residual internal stresses were estimated thanks to XRD measurements, by using the "$\sin^2(\psi)$" methodology [69].

As-received coating hardness were evaluated using micro- and nano-hardness measurements with Vickers or Knoop indenters. It can be mentioned that such measurements were also used after ion irradiation of Cr-coated Zircaloy-4 to quantify the irradiation hardening of the Cr coating at 400 °C [70]. For particular cases, additional "scratch tests" measurements were performed to get complementary information on the adhesion of the coating to the substrate.

Additionally, tensile tests were conducted at Room Temperature

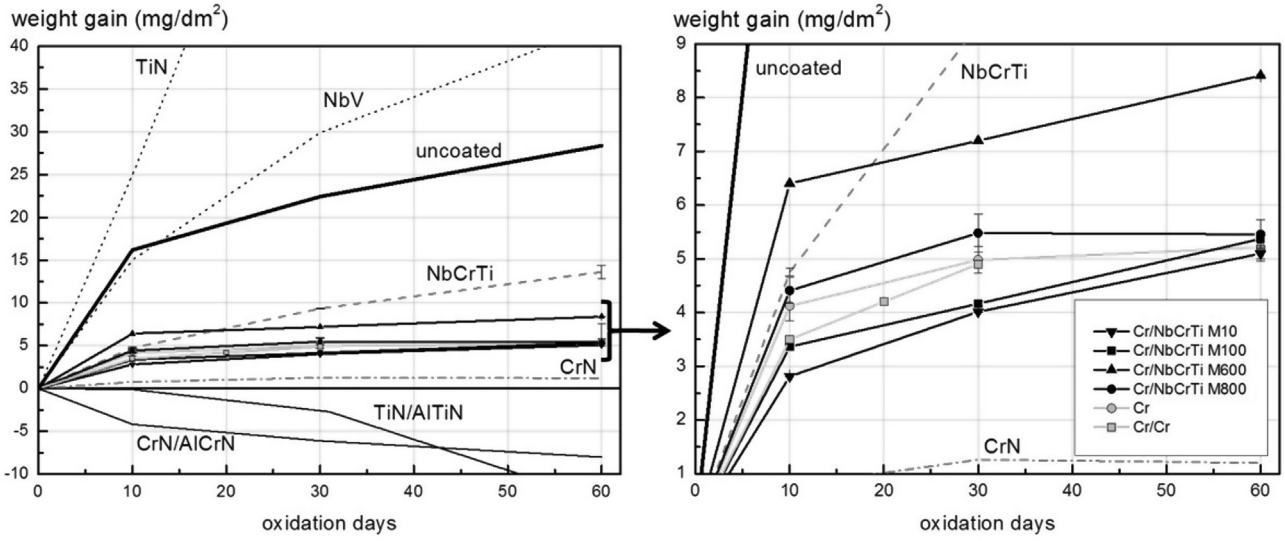


**Fig. 1.** Weight gain evolution as a function of oxidation time of several coated Zircaloy-4 sheets samples after autoclave tests performed at 360 °C in pressurized water with typical PWR primary water chemistry 21.

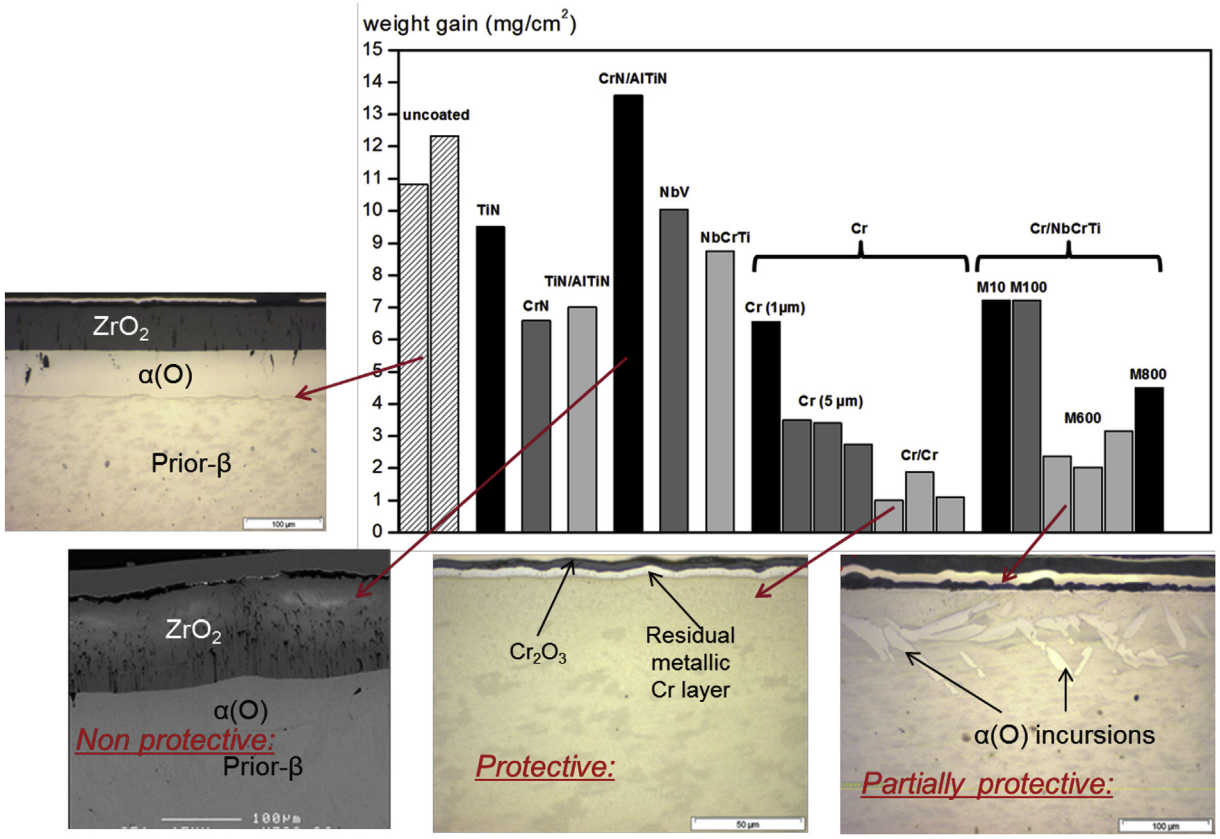


**Fig. 2.** Weight gain and typical optical micrographs of a transverse cross-section obtained on several coated Zircaloy-4 sheets samples after HT steam oxidation for 850 s at 1100 °C and direct water quenching down to RT 21.

(RT) on 1.2 mm-thick, 4 mm-wide and 17 mm-long gauge samples. These tests were carried out on an INSTRON 5966 10 KN tensile device, with a prescribed displacement rate of $8.5 \times 10^{-3}$ mm $s^{-1}$, *i.e.* an initial average strain rate of approximately $5 \times 10^{-4}$ $s^{-1}$. To assess the failure mode of the samples, fracture surfaces of the samples were examined by Scanning Electron Microscopy (SEM).

### 2.3. Corrosion testing (360–415 °C)

Coated samples were (out-of-pile) tested in autoclave. The early tests were carried out in static autoclaves at 360 °C and 18.7 MPa in static water with a typical Pressurized Water Reactor (PWR) primary water chemistry. The primary water chemistry is composed of 10 wt ppm of lithium and 650 wt ppm of boron issued, from, respectively, lithium hydroxide and boric acid. More recent tests were performed in steam at 415 °C pressurized at 100 bar to accelerate the corrosion rate. Periodic visual examination, weight measurement and hydrogen content measurement (on samples, including oxide layers, extracted from the corroded specimens, by using an inert gas fusion thermal conductivity technique) were made. Post-test optical and SEM examinations were conducted to get some insights into the outer oxide growth.

### 2.4. Preliminary fretting/wear tests (PWR environment)

Preliminary fretting/wear tests were performed in the "FROTTEAU 2" wear test rig, having reciprocating sliding horizontal motion. This wear machine operates in primary PWR conditions, with circulating water parallel to the axis of motion. Excitation was provided by an eccentricity and crank arrangement. The motion was transmitted to the test specimen inside the rig by a shaft driven by an external electro-magnetic device.

For the test described here, a 77 mm-long Zr rod was connected to the shaft and was the movable lower part. A 20 mm-long Zr plane support was linked above the rod on a supporting system and the normal force was obtained by the total dead weight ($3 \pm 0.1$ N, measured in static water at room temperature). Two identical rod/support testing devices were mounted and permitted two wear results per test.

### 2.5. High temperature oxidation (LOCA)

Oxidation tests were carried out in pure flowing steam (atmospheric pressure, steam flow rate normalized to the cross-sectional area of the steam chamber of approximately 70 mg/($cm^2$·s)) at 1000, 1100 and 1200 °C thanks to the CEA's "DEZIROX 1" facility [71–74]. This facility is considered as a reference device at CEA for HT steam oxidation. It has been extensively used in the past two decades to assess the behavior of modern Zr based nuclear fuel claddings. Indeed, more than two thousands HT oxidation tests have been conducted so far and a huge HT oxidation database is thus available. At the end of the isothermal oxidation step, direct water quenching was applied down to Room Temperature (RT). Such final cooling conditions are expected to be conservative when compared to more prototypical LOCA transients including a two-step cooling scenario (*i.e.*, cooling at an intermediate cooling rate (1–10 °C/s) down to an intermediate temperature (700–800 °C) from which the final water quenching is applied down to RT [75–77]). In fact, it has been observed that a two-step final cooling scenario may induce a higher PQ clad ductility when compared to direct quenching [73–78].

Post-Quenching (PQ) metallurgical examinations including Electron Probe Micro-Analysis (EPMA, CAMECA SX100 electron microprobe) was carried out to get additional insights into the coated claddings oxidation behavior and the capacity of the coating to delay the oxygen diffusion into the Zircaloy-4 matrix, which is known to be one of the main parameters responsible for the PQ clad embrittlement [73,79–81].

## 3. Results and discussion

### 3.1. Early screening tests on several types of PVD coating

*Corrosion in nominal conditions* – Fig. 1 illustrates the weight

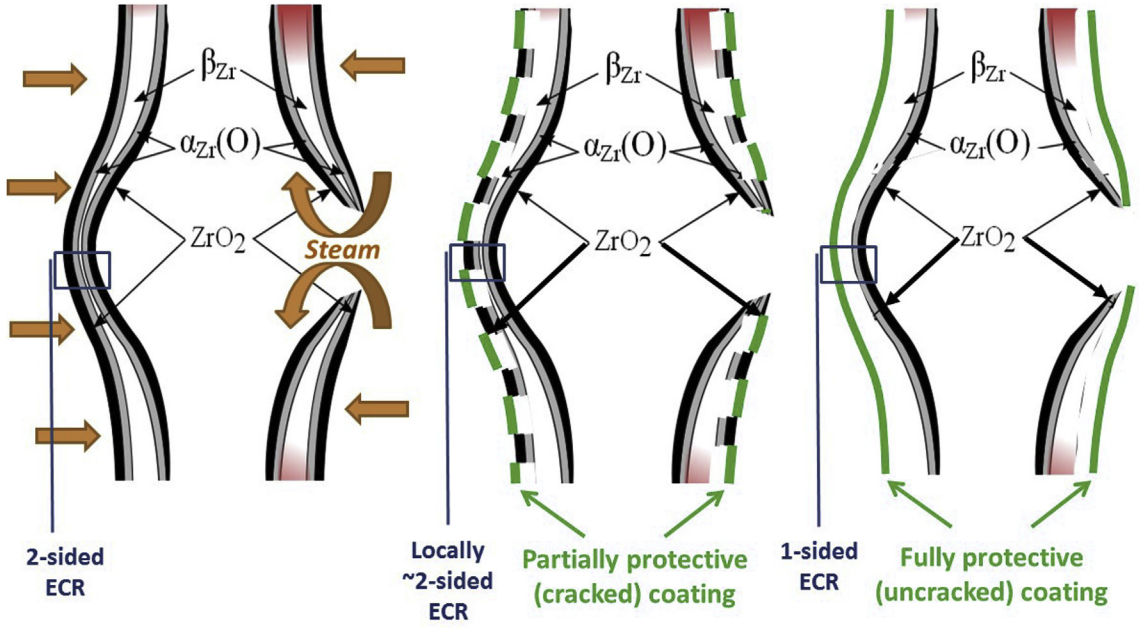


**Fig. 3.** Schematic representation of the behavior of the outer coating upon HT steam oxidation in the vicinity of the clad balloon following internal pressure-induced burst (LOCA) 22.

gain evolution of several coated Zircaloy-4 sheets samples after autoclave tests performed at 360 °C in pressurized water for typical PWR primary water chemistry. According to these curves, the best behavior is observed for CrN, Cr, Cr/Cr and multilayered Cr/NbCrTi coatings, while TiN and NbV coatings show the poorest behavior. Moreover, a loss of weight gain is observed for Al-containing multilayered coatings. For these last coating materials, it is likely that the observed weight gain evolution is due to outward migration of aluminum and potential release in the pressurized water, as already observed in Refs. [18,20,32]. Such a behavior is questionable since the industrial PWR chemistry specifications are very restrictive and do not allow significant chemical species release from the internal core materials. Indeed, such a phenomenon may induce redeposition in some (colder) parts of the primary PWR loop circuit, activation of the filters, etc … Additionally, as observed during in-reactor corrosion loop tests in the HALDEN reactor [32], aluminum-containing coatings may totally disappear after having experienced corrosion under normal operating conditions including neutron irradiation. Thus, (TiN,CrN)/AlTiN coatings seem to be unsuitable for application to LWR nuclear fuel claddings.

*HT oxidation behavior (LOCA)* – Fig. 2 shows the weight gain and typical optical micrographs obtained on the different coated Zircaloy-4 sheets samples after steam oxidation for 850 s at 1100 °C and direct water quenching down to RT (LOCA conditions). This HT oxidation time-temperature condition corresponds to typical Equivalent Cladding Reacted (ECR) values of ~10–11% using the Baker-Just [84] correlation for two-sided oxidation of 1.2 mm-thick uncoated Zircaloy-4 sheets, as tested here (more or less

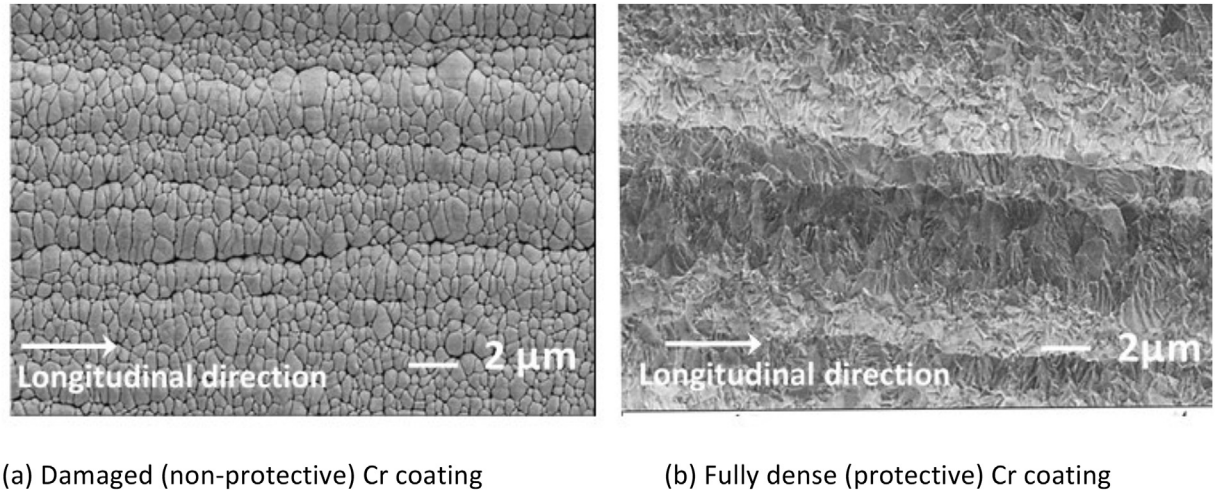


**Fig. 4.** SEM micrographs of the surface of as-received Cr-coatings on Zircaloy-4 sheet substrate 22.

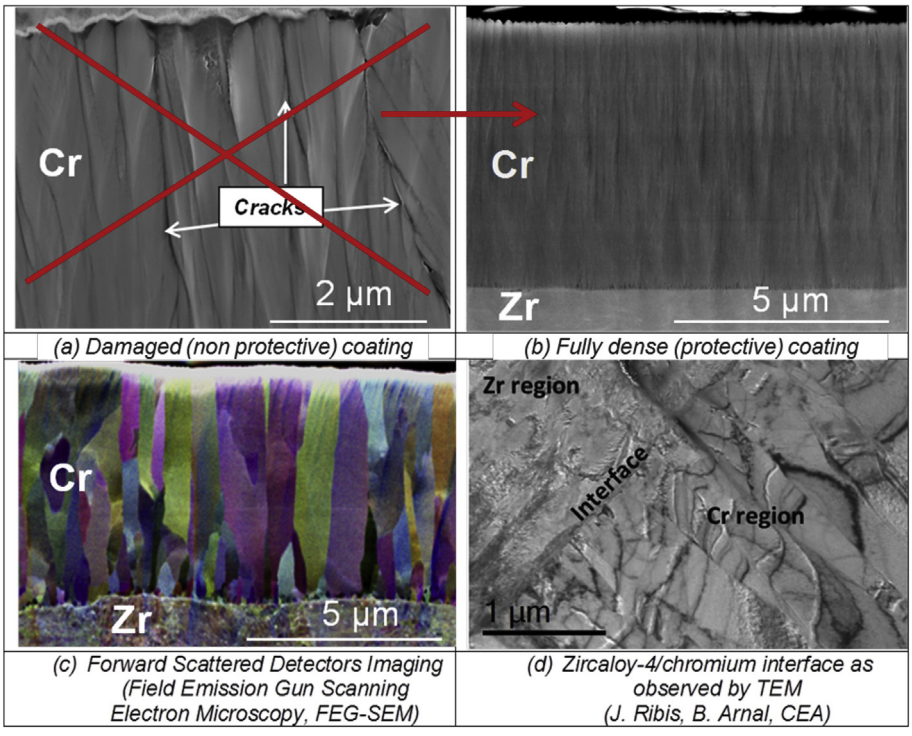


**Fig. 5.** Typical as-received microstructure of PVD Cr coatings on Zircaloy-4 substrate 23.

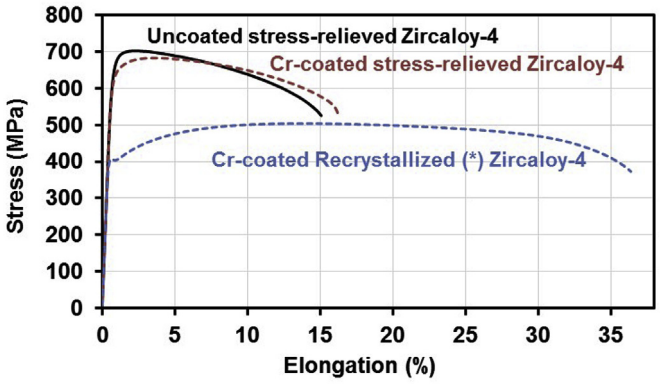


*(*)Zircaloy-4 substrate recrystallized due to not convenient PVD deposition parameters*

**Fig. 6.** Engineering tensile curves obtained at RT on uncoated and Cr-coated Zircaloy-4 (sheet samples) 24.

representative of the ECR corresponding to one-sided oxidation of a 0.6 mm-thick cladding).

From these results, the best behavior (lower weight gain) is observed for ("PVD multipass") Cr/Cr coatings while PVD monolayer Cr coatings are not fully protective. Indeed, for the HT oxidation conditions tested here, Cr/Cr coatings exhibit a continuous residual metallic chromium layer beneath the outer chromia ($Cr_2O_3$) layer with no indication of significant oxygen ingress into the Zircaloy-4 substrate. Thus, they can be considered as fully protective. Cr/NbCrTi coatings exhibit an intermediate behavior with indication of oxygen diffusion into the Zircaloy-4 prior-$\beta_{Zr}$ substrate as highlighted by the discontinuous growth of oxygen-stabilized $\alpha_{Zr}(O)$ incursions. This means that for this particular case, oxygen diffusion has occurred across the residual non oxidized, intermediate, coating metallic layer but the net flux of oxygen into the Zircaloy-4 matrix was not high enough to induce formation of fresh zirconium oxide beneath the coating tested.

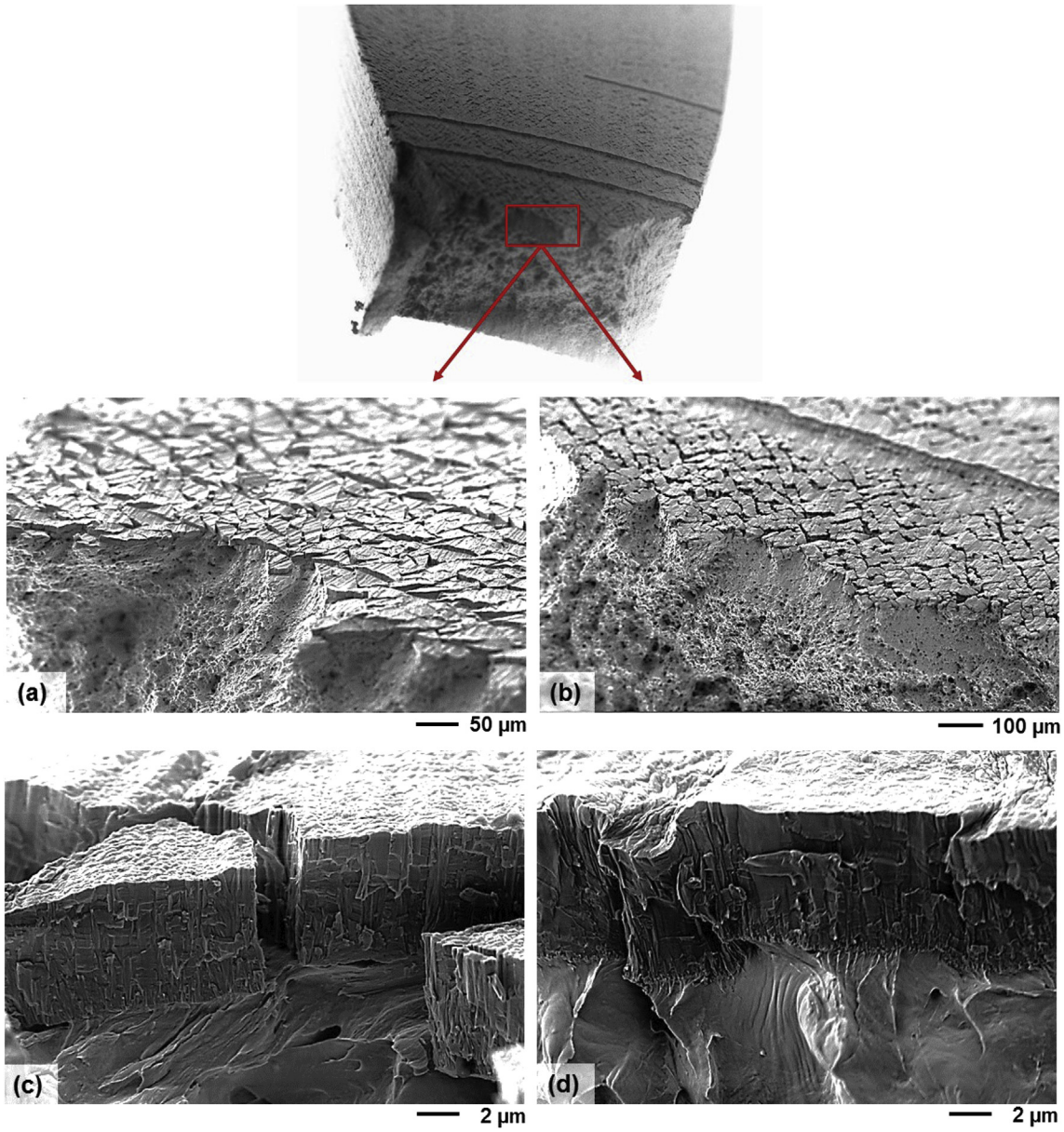


**Fig. 7.** Typical SEM fractogaphs of Cr-coated Zircaloy-4 samples tensile-tested at RT LEFT: (a) & (c) - poorly ductile and partially spalled Cr-coating RIGHT: (b) & (d) – more ductile and very well bonded Cr-coating 25.

Finally, a poor oxidation behavior is observed for most of the ceramic (nitrides) coatings. For one extreme case, *i.e.* for Cr/AlTiN coating, the final weight gain is even slightly higher than the one of reference uncoated Zircaloy-4, consistently with the formation of a thicker outer zirconium oxide. Nevertheless, a rigorous comparison of the HT steam oxidation behavior of the different coatings tested here is not possible due to the various initial thicknesses of the coatings (and probably not fully optimized deposition parameters at this early stage of coatings developments). It is likely that some of the coatings tested were not thick enough to undergo steam oxidation for 850 s at 1100 °C.

Considering their good corrosion behavior in both nominal and LOCA (HT steam) conditions, chromium-based coatings were selected for further development and evaluation. One additional motivation for choosing a fully metallic-based coating was its intrinsic ductility at HT when compared to ceramic (nitrides) coatings. Indeed, in LOCA conditions, the nuclear fuel cladding may experience significant strain (ballooning) due to the internal clad pressure and to the temperature increase inducing accelerated viscoplastic strain. For example, internal pressure burst tests have been conducted recently on CrN-coated Zr based claddings at ORNL [9]. They have shown that the ceramic chromium-nitride coating did not sustain the clad circumferential elongation at the balloon location, inducing a high surface density of open cracks. It is believed that such a high damage of the coating may drastically limit the protective property of the coating against subsequent HT steam oxidation.

At that point, one could argue that, upon prototypical LOCA transient and after significant ballooning, cladding burst may occur and then, the inner uncoated surface of the clad would be exposed to steam. However, even if cladding burst occurs and as shown schematically in Fig. 3, it is still interesting to maintain the outer oxidation resistance to avoid extended two-sided oxidation. Indeed, preserving the outer coating efficiency should induce one-sided (inner clad) oxidation conditions. In such conditions and taking into account that the HT oxidation kinetics of the zirconium matrix is more or less parabolic, one could expect an oxidation time before achieving full cladding embrittlement more or less four times longer, when compared to two-sided oxidation which could take place at the location of cracks in the outer (deformed) coating.

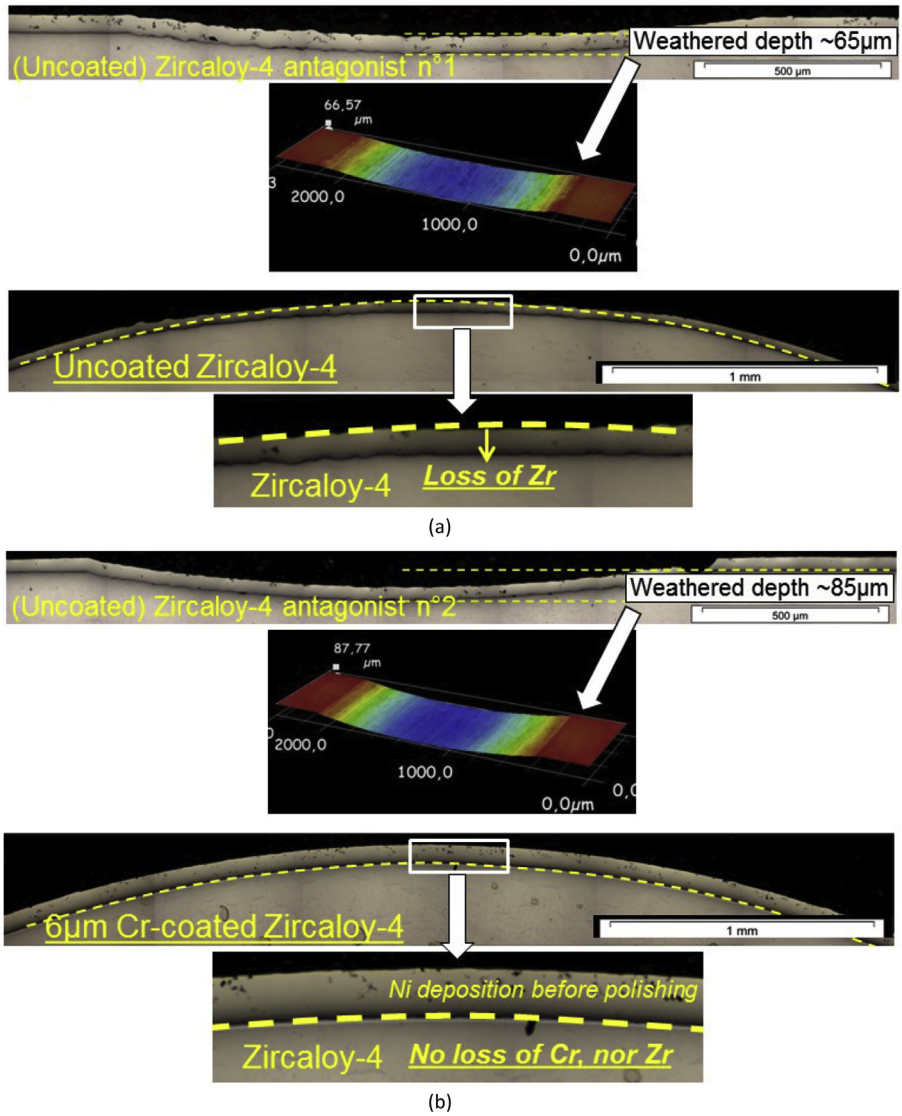


**Fig. 8.** Optical (2D and 3D) views of the tested uncoated and 6 µm Cr-coated Zircaloy-4 clad segments and their respective (uncoated Zircaloy-4 plates) antagonists, after fretting/wear testing (320 °C, 155 bar pressurized water, PWR chemistry, linear load applied = 150 N/m, 3600 cycles, total time = 2 h, cumulative slide length ~160 m) 26.

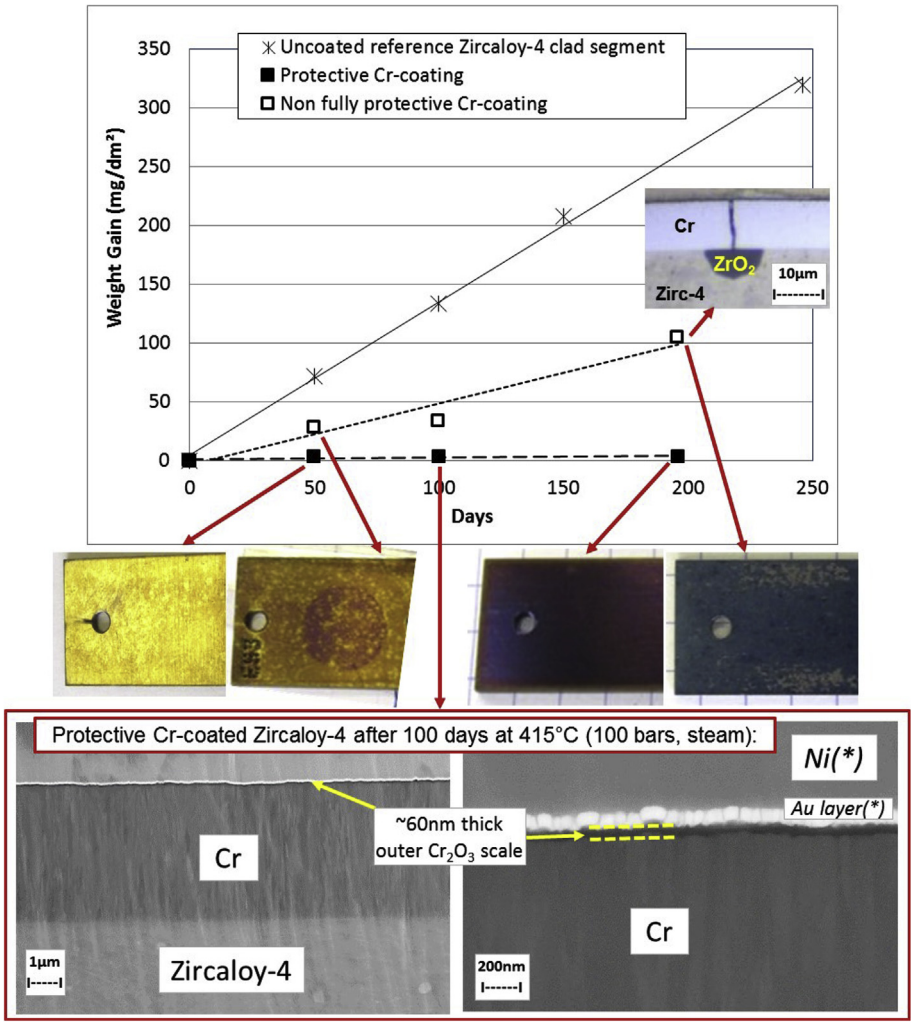


**Fig. 9.** Weight gain evolution, typical macroscopic aspects and SEM electron micrographs of uncoated and Cr-coated Zircaloy-4 sheet samples after autoclave tests in steam at 100 bar and 415 °C (*) *Au and Ni outer layers deposited just before polishing to preserve the thin outer $Cr_2O_3$ scale* 27.

Finally, concerning protection of the clad inner surface against incidental oxidation due to leaking fuels rods or occurring after HT (LOCA) burst occurrence, it must be mentioned that recent efforts were made at CEA in collaboration with french universities to develop a process able to coat efficiently the clad inner surface. First results obtained using a special chemical vapor deposition process and an amorphous chromium carbide inner coating are encouraging, showing significant protection of the clad inner surface upon HT steam oxidation [82].

### 3.2. First generation of 5–10 µm-thick Cr-coated Zircaloy-4

#### 3.2.1. As-received microstructure and properties

Microstructure and properties of the as-received coating depend on the coating materials, on the process/deposition parameters and on the coating thickness. Fig. 4 and Fig. 5 show typical microstructures of as-received Cr coatings. By using convenient deposition PVD process and parameters, it was possible to obtain fully dense coating without evidence of cracks and/or interface debonding. Micrograph (c) of Fig. 5 illustrates the typical elongated morphology of Cr grains resulting from the PVD process. From X-ray and EBSD measurements, it was noticed that the Cr (body-centered cubic, bcc, lattice) coatings generally exhibit a predominant [100] fiber crystallographic texture normal to the surface, with sometimes a second [111] component. Some published data also mentioned a [110] fiber crystallographic texture for Cr coatings deposited by PVD on other substrate materials [87], the (110) plane corresponding to the plane of highest density. From XRD measurements, compressive residual internal stresses parallel to the surface are generally observed, with stress levels ranging from a few tens up to a few hundreds of MPa. It is believed that such a compressive internal stress state should contribute to the good mechanical behavior of the coating[5].

Depending on the PVD deposition parameters and the coating thickness, micro/nano-hardness measurements gave values ranging from ~300 up to more than 1000HV (Vickers Hardness), which is consistent with some hardness measurements already made on Cr-coating on other substrates [84–86]. As for other coating materials, such a wide range of hardness should be related to the coating internal stresses and grain sizes ("Hall & Petch" effect). Scratch tests were also carried out, evidencing no early coating delamination or spallation, thus indicating a good Cr-Zircaloy-4 bounding. In-depth HRTEM examinations and micro-analysis showed that the Cr-Zircaloy-4 interface is constituted of

[5] As for other coated materials, strong internal tensile stresses have to be avoided because they could contribute to incipient cracking of the coating, as already observed in Ref. [88] on Cr-electroplated coatings.

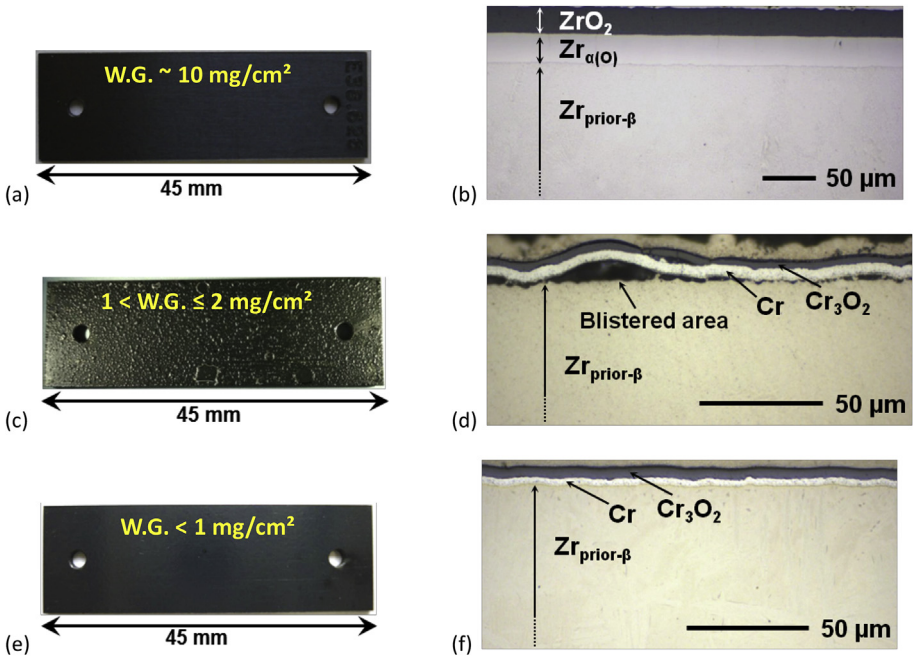


**Fig. 10.** Macrographs of the surface and optical micrographs of polished cross-section of (a, b) uncoated, (c, d) not fully protective Cr-coated, and (e, f) fully protective Cr-coated Zircaloy-4 (sheet samples) after steam oxidation for 300 s at 1200 °C followed by direct water quenching 28.

nanometric $Zr(Cr,Fe)_2$ intermetallic sublayers with crystallographic continuity between the different interphase interfaces [67]. Additionally, it was shown that this continuity is kept after ion irradiation [68,70]. Thus, it is expected that the Cr-coating bounding strength will be maintained after in-reactor irradiation, as recently observed for neutron irradiated Cr-coated Zr based alloys [10].

Tensile tests were carried out at RT on both reference (stress-relieved) and Cr-coated Zircaloy-4 sheet samples. Fig. 6 displays typical engineering stress-strain curves obtained for uncoated and Cr-coated Zircaloy-4. It can be observed that care has to be taken during the deposition process to limit temperature of the substrate and thus avoid any modification of the as-received clad material properties. Thus, by using convenient PVD process and adequate deposition parameters and, as already mentioned in Ref. [57] for the last generation Cr-coated M5 substrate, the Cr-coating process does not modify the mechanical properties of the as-received uncoated reference cladding material, as highlighted by the red dotted curve in Fig. 6. Moreover, it can be mentioned that mechanical strength of pure chromium at temperatures ranging from RT up to at least in-service cladding temperatures, *i.e.* approximately 350 °C [89], is not very different from that of industrial Zr-based alloys. Thus the thin outer chromium layer is unlikely to significantly impact the overall clad mechanical properties in nominal conditions. However, as shown in some other papers [56,59,62], this is not the case for higher temperatures – typical of hypothetical LOCA conditions – at which a strengthening effect of the Cr coating is observed.

Typical post-tensile test SEM fractographs are shown in Fig. 7 for zones where stress triaxiality and plastic strain were high. The reduction of area at fracture is beyond 40%. Even if it is cracked, the outer chromium layer[6] is still adherent to the substrate, thus confirming the good bonding strength of the Cr-Zircaloy-4 interface. Electron micrographs on the left in Fig. 7 correspond to a Cr-coating with limited ductility, locally debonded from the substrate due to non-optimized deposition parameters. When using adequate PVD process and deposition parameters, the Cr coating shows high bonding strength and limited cracking, even within the highly deformed zones, as highlighted by the SEM micrographs on the right in Fig. 7.

As previously mentioned, preliminary fretting/wear tests were also carried out on uncoated and ~6 µm-thick Cr-coated Zircaloy-4 clad segments. The test conditions applied here were very aggressive as compared to more realistic in-reactor fretting conditions which can take place within the nuclear fuel subassembly, due to grid-to-rod and potential debris fretting effects. Thus, the results have to be considered as very conservative. Fig. 8 shows the post-test aspects of the tested uncoated and 6 µm Cr-coated Zircaloy-4 clad segments and their respective (uncoated Zircaloy-4 plates) antagonists. For the severe fretting/wear conditions applied, a significant loss of zirconium is observed on both the uncoated Zircaloy-4 segment and on the (uncoated) antagonist counterpart samples. For the last ones, the cumulative wear depth ranges from −65 µm to −85 µm.The outer surface of the 6 µm Cr-coated sample was remarkably not affected, with no indication of loss of Cr (or Zr). Such a result was recently confirmed on the last generation of 10–20 µm Cr-coated M5 for more representative PWR fretting/wear conditions applied [58]. It is thus expected that the use of hard and strongly adherent Cr-coating on zirconium-based claddings should contribute to reduce significantly grid-to-rod and debris fretting clad failures for in-reactor conditions, thus limiting drastically the potential occurrence of leaking fuels.

### 3.2.2. *Corrosion behavior of 5–10 µm Cr-coated Zircaloy-4 in nominal conditions*

Short and preliminary corrosion tests have been carried out on first generation of Cr-coated Zircaloy-4 sheet samples in pressurized water (PWR chemistry) at 360 °C in autoclave up to 60 days.

[6] Due to its bcc crystallographic structure, chromium is characterized by a relatively high ductile-to-brittle transition temperature, inducing a macroscopic brittle behavior when tested at low temperatures (at temperatures lower than ~100 °C typically) [89,90]. Hopefully, for higher temperatures, ductility of chromium is significantly enhanced [89].

Even if this very first generation of Cr coatings was not fully protective, it was observed that the Cr-coating enhances the overall corrosion resistance when compared to the uncoated reference Zircaloy-4. In a second step, a second generation of Cr-coated Zircaloy-4 were tested in steam at 415 °C pressurized at 100 bar to accelerate the corrosion rate, for longer autoclave testing times (up to 200–250 days). Fig. 9 gives an overview of some of the results obtained. It can be observed that:

- The outer surface color of the coated materials evolves from gold to magenta/deep blue for autoclave duration ranging from a few tens of days up to 200 days. Such color evolution is linked to the growth of the thin chromia ($Cr_2O_3$) outer scale. For not fully protective Cr-coatings, grey spots are observed at the surface of the sheet samples. This is likely due to the local formation of zirconia ($ZrO_2$) oxide "islands", as discussed hereinafter.
- When appropriate PVD process and deposition parameters are used, the Cr-coating is remarkably protective with very low weight gain values: less than 5 mg/dm$^2$ to be compared to more than 260 mg/dm$^2$ for the uncoated reference Zircaloy-4 after 200 days of autoclave testing at 415 °C. This last weight gain value corresponds to the formation of a ~17 μm-thick zirconia scale, while high magnification SEM examinations showed that, for fully protective Cr-coating, the outer chromia ($Cr_2O_3$) thickness was lower than 100 nm after 100 days of autoclave testing (Fig. 9). Thus, if such a behavior is confirmed under neutron irradiation, one could expect negligible corrosion of Cr-coated nuclear fuel claddings for in-reactor conditions.
- Additionally, attention has to be paid to the effects of hypothetical localized through-thickness cracks in the coating which could induce localized accelerated oxidation of the substrate and/or Cr-coating spallation. Thus, it was decided to test simultaneously some Cr-coated samples with initial defects introduced intentionally within the Cr-coating, by using degraded PVD deposition parameters. Those samples are labelled as "not-fully-protective" in Fig. 9. In this figure, the upper right optical micrograph shows a typical zirconia island beneath the outer Cr-coating layer due to a pre-existing through-wall crack in the Cr-coating. It is interesting to observe that there is no experimental evidence here of local spallation of the Cr coating in the vicinity of the underneath zirconia oxide spot (taking into account that zirconia oxide formation may induce a (localized) volume expansion of nearly 50%, corresponding to the so-called "Pilling-Bedworth" ratio). Moreover, the actual thickness of zirconia is lower than 10 μm while zirconia thickness formed in the same conditions on uncoated reference Zircaloy-4 is twice larger. This indicates that no localized oxidation acceleration has occurred. Such an acceleration may have been eventually expected due to local electrochemical "galvanic-couple" effects at the Zr-Cr bonding interface. As illustrated at the end of the next section, this last result also stands for HT steam oxidation in LOCA conditions.

*Hydrogen uptake* – One well-known negative consequence of in-reactor corrosion of zirconium-based nuclear fuel claddings is the associated hydrogen uptake which may induce cladding embrittlement due to the detrimental effects of precipitated hydrides within the zirconium matrix. Thus, hydrogen analyses were carried out on several autoclave-tested Cr-coated samples and compared with results obtained on the uncoated reference material. The

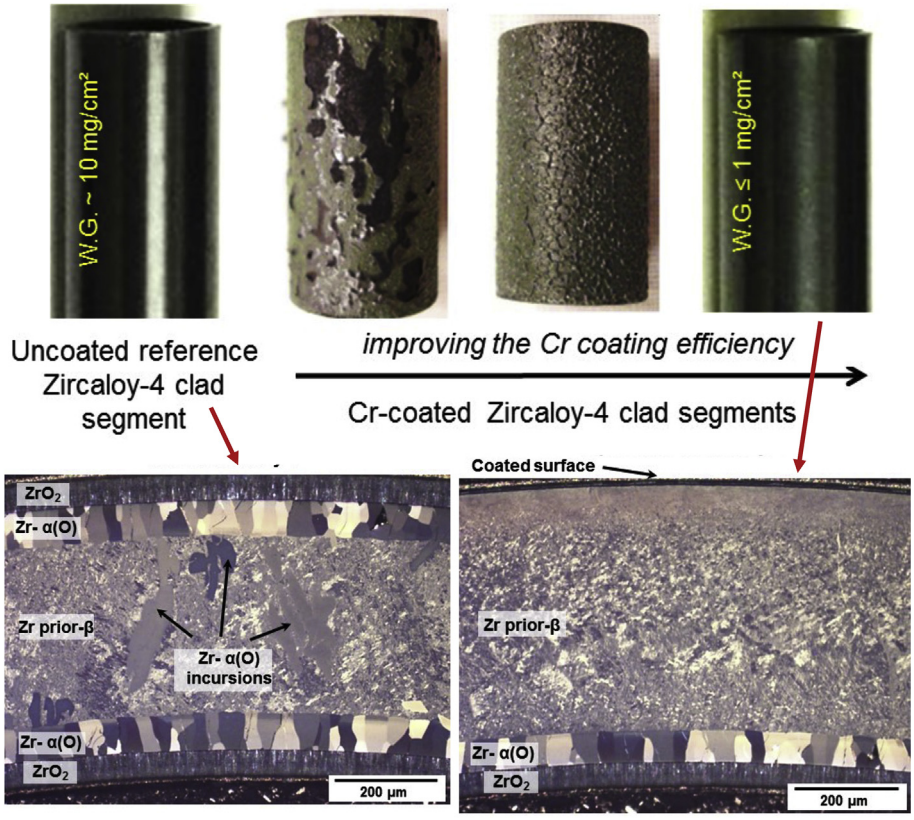


**Fig. 11.** Macrographs and optical (polarized light) of uncoated/Cr-coated Zircaloy-4 clad segments after steam oxidation for 300 s at 1200 °C followed by direct water quenching *Remark: because of the two-sided oxidation conditions applied, for the coated clad, the weight gain has been evaluated by subtraction of the contribution of the uncoated inner surface (calculated using the weight gain measured for the uncoated reference)* 29.

measured hydrogen concentration reached around 1000 wt.ppm after 200 days for uncoated Zircaloy-4 (the hydrogen pick-up ratio is higher in steam at 415 °C than in pressurized water at 300–360 °C), while for the same testing conditions, the hydrogen contents of not fully protective and fully protective Cr-coated samples reached ~150 and ~25 wt.ppm respectively. If confirmed for fully representative PWR in-reactor environment, this result suggests that as far as efficient deposition process and parameters are used, Cr-coated Zr-based nuclear fuel claddings would be an efficient mitigation solution against hydriding due to the in-service clad corrosion. This would increase the robustness of the nuclear fuel clad not only upon nominal in-service conditions but also in hypothetical accidental situations (LOCA, reactivity initiated accident, …). This may also induce some benefits for post-service nuclear fuel subassembly handling, storage and transportation issues.

### 3.2.3. HT steam oxidation behavior of 1st generation of 5–10 μm Cr-coated Zircaloy-4 (representative of DBA-LOCA and slightly beyond conditions)

HT steam oxidation tests were performed within the 1000–1200 °C temperature range for DBA-LOCA and slightly beyond oxidation times. As a first step, to monitor the Cr PVD process and deposition parameters in order to obtain efficient resistance to HT oxidation, a first set of tests was carried out for 300 s at 1200 °C on several Cr-coated sheet samples fabricated through different coating process routes. This HT oxidation condition was chosen because, for the sheet and clad sample thicknesses considered here, it corresponded to typical one-sided and two-sided oxidation "Baker-Just" ECR values of nearly 12 and 22.5% respectively. The historical regulatory ECR LOCA criteria of 17% is therefore within the ECR values interval tested here. The experiments were carried out on both Cr-coated sheets and tubular clad segments, as shown respectively in Fig. 10 and Fig. 11.

When appropriate PVD process and deposition parameters are applied, it can be observed that 5-10 μm-thick Cr coatings lead to a decrease of the weight gain by at least a factor ten when compared to the reference uncoated material. This reduction in oxidation in the presence of Cr coating for DBA-LOCA oxidation times and temperatures is qualitatively consistent with some recent results obtained by other institutes on Cr and CrN coated zirconium-based claddings [4,14,16,17,21,28,44,45], even if some of the mentioned results sometimes differ, likely due to different process/deposition parameters.

Additionally, to get some insights into the HT oxidation behavior of the Cr coatings, Fig. 12 shows typical electron SEM micrographs and associated EPMA profiles across the sub-oxide residual metallic (non-oxidized) chromium layer, for two Cr-coated Zircaloy-4 sheets after steam oxidation for 300 s at 1200 °C. The first coating shows numerous pores and extended defects at the Zr/Cr interface after the HT oxidation test. It is then obvious from the associated EPMA measurements that oxygen has diffused through the chromium wall thickness confirming the non-protective behavior of this particular sample. On the contrary, the second sample obtained with convenient Cr deposition process/parameters shows no pores/defects nor indication of oxygen ingress into the residual metallic chromium beneath the outer chromia scale, thus confirming a fully protective behavior, in agreement with the low weight gain measured (lower than 1 mg/cm$^2$). Moreover, for both oxidized coatings, a ~1 μm-thick $ZrCr_2$-type intermetallic has grown at the Cr/Zr interface. As mentioned earlier, such an intermetallic phase at the interface was already present in the as-received state but with a nanometric thickness. In fact, consistently with the Zr-Cr phase diagram, a $ZrCr_2$ type intermetallic layer has grown at the Cr/Zr interface due to Cr-Zr inter-diffusion which took place during HT oxidation. One may notice from the EPMA results (Fig. 12) that this

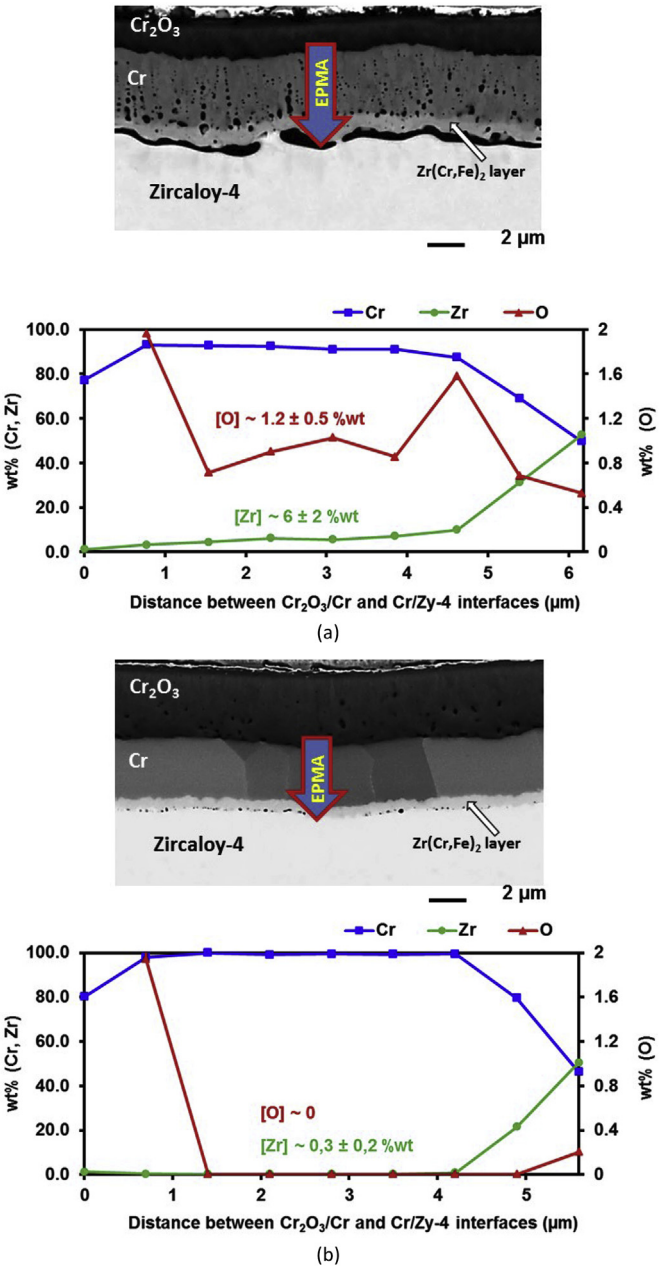


**Fig. 12.** Typical electron SEM micrographs and associated EPMA profiles across the residual non-oxidized chromium layer of (a) not fully and (b) fully protective Cr-coated Zircaloy-4 sheets after steam oxidation for 300 s at 1200 °C, followed by direct water quenching 30.

thin intermetallic layer is slightly enriched in iron. It is likely that this iron enrichment came from the dissolution at HT of the Laves $Zr(Fe,Cr)_2$ precipitates initially present within the $\alpha_{Zr}$ Zircaloy-4 matrix. This observation confirms the high thermodynamic affinity of iron to the Cr/Zr interface intermetallic layer also evidenced before and after ion irradiation at 400 °C of Cr-coated Zircaloy-4 [67,68,70].

Fig. 13 summarizes the weight gain evolution of uncoated and several of the first generations of 5–10 μm Cr-coated Zircaloy-4 sheet samples as a function of the square root of time, up to 450 s at 1200 °C. This figure shows that for these typical DBA-LOCA oxidation times, the oxidation kinetics of Cr-coated Zircaloy-4 is nearly parabolic and much slower than the one of the reference uncoated

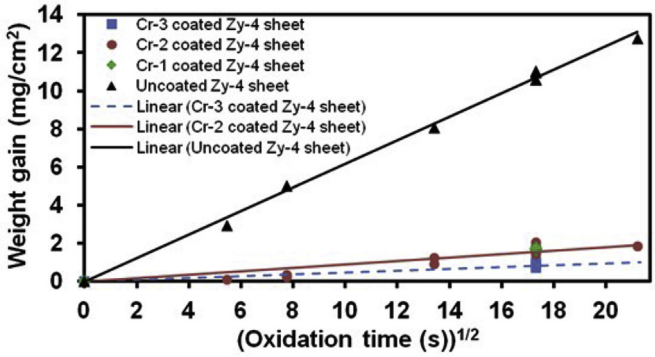


**Fig. 13.** Weight gain evolution as a function of the square root of oxidation time in steam at 1200 °C of uncoated and Cr-coated Zircaloy-4 sheets (for typical DBA-LOCA oxidation times) 31.

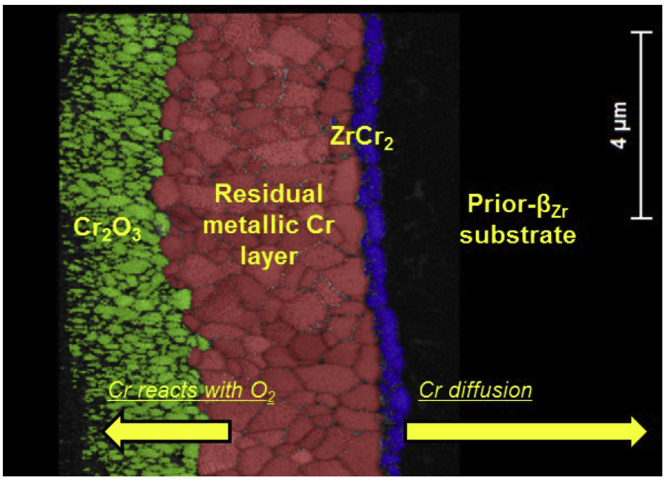


**Fig. 14.** SEM-EBSD map in phase contrast imaging mode of a Cr-coated Zircaloy-4 sheet sample after steam oxidation for 300 s at 1200 °C 31.

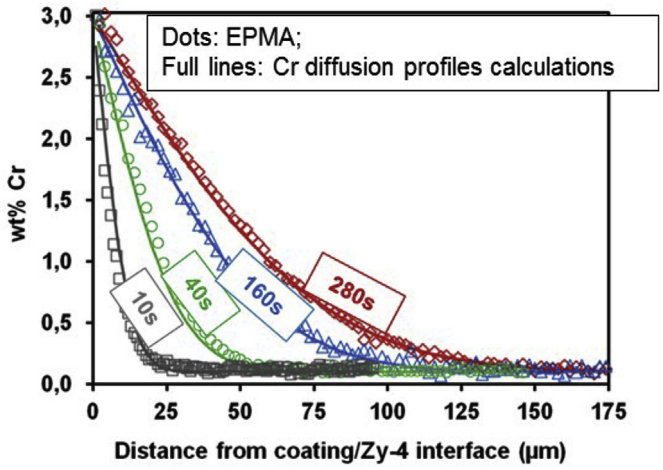


**Fig. 15.** Experimental (EPMA) and calculated Cr diffusion profiles into the prior-$\beta_{Zr}$ substrate from the Zr/Cr interface after steam oxidation at 1200 °C 32.

Zircaloy-4. Then from equation (1), the Kp parabolic constant values derived from Fig. 13 are ~0.62 mg/cm$^2$/s$^{1/2}$ and ~0.05 mg/cm$^2$/s$^{1/2}$, for uncoated and Cr-coated sheets Zircaloy-4 respectively. Then, it is possible to calculate the outer chromia thickness from

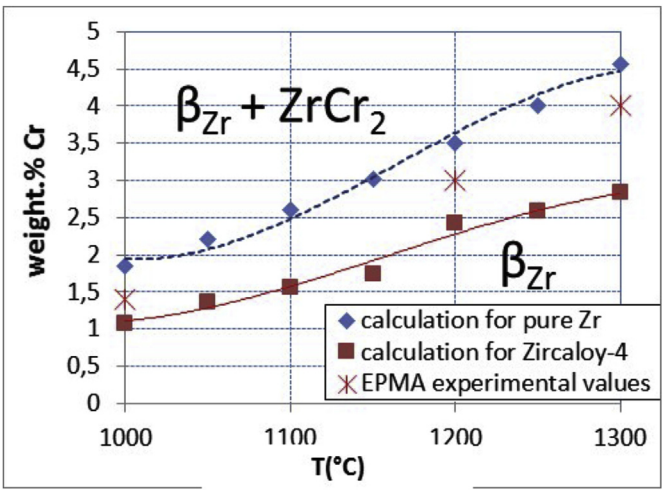


**Fig. 16.** Calculated (Thermocalc® + Zircobase) evolution of the chromium solubility within the HT $\beta_{Zr}$ phase in equilibrium conditions for pure binary Zr-Cr and pseudo-binary Zircaloy-4-Cr systems, compared to experimental (EPMA) data 32.

the weight gain measured, assuming that all the oxygen which has reacted with the Cr-coating has transformed into stoichiometric $Cr_2O_3$ oxide[7] (for the oxidation conditions considered here, the potential fraction of volatilized Cr has been neglected). Finally, from the chromia thickness evaluation, one can deduce the equivalent thickness of metallic chromium consumed by the outer chromium oxide scale formation.

$$\text{Weight Gain (mg/cm}^2) = \text{Kp.[oxidation time(s)]}^{1/2} \quad (1)$$

*Overall Cr-coating consumption kinetics in oxidizing environment at HT* – As an EATF clad concept, the Cr coating plays a sacrificial role upon HT oxidation until its full "consumption". Thus, thanks to its lower oxidation rate compared to uncoated Zircaloy-4 and as far as convenient deposition process/parameters have been used to obtain a fully dense, adherent and protective chromium scale, the Cr-coating may induce an additional "grace period" before the full clad embrittlement is achieved. In fact, as highlighted by Fig. 14 and Fig. 15, the overall Cr-coating consumption kinetics in steam at HT is not only due to the formation of an outer chromia scale but also results from the simultaneous chromium diffusion into the underlying $\beta_{Zr}$ substrate. Such phenomenon is due to the increase in chromium solubility within the HT $\beta_{Zr}$ phase as the temperature increases. As shown in Fig. 16, thermodynamic calculations using Thermocalc® [92] associated with the CEA "Zircobase" thermodynamic database [93,94] predict that the Cr solubility in Zircaloy-4 may achieve ~2.5 wt % (wt.%) at 1200 °C, while an experimental value of ~3 wt% was determined from the EPMA Cr profile measurements (Fig. 16), assuming local thermodynamic equilibrium at the $ZrCr_2/\beta_{Zr}$ interface. Then, it is possible to calculate the Cr diffusion profiles using the analytical "Fick" law solution for one dimension semi-infinite (volume) thermal diffusion of Cr within the $\beta_{Zr}$ phase at HT (Equation (2)):

$$[C(x,t)-C_o] = [C_s-C_o].(1-\text{erf}(x/(2\sqrt{Dt}))) \quad (2)$$

[7] Let us recall that such an assumption is not valid for uncoated Zirconium-based claddings because, at HT, a significant part of the oxygen coming from the outer steam oxidation diffuses into the $\beta_{Zr}$ substrate forming an oxygen-stabilized $\alpha_{Zr}(O)$ sub-oxide layer.

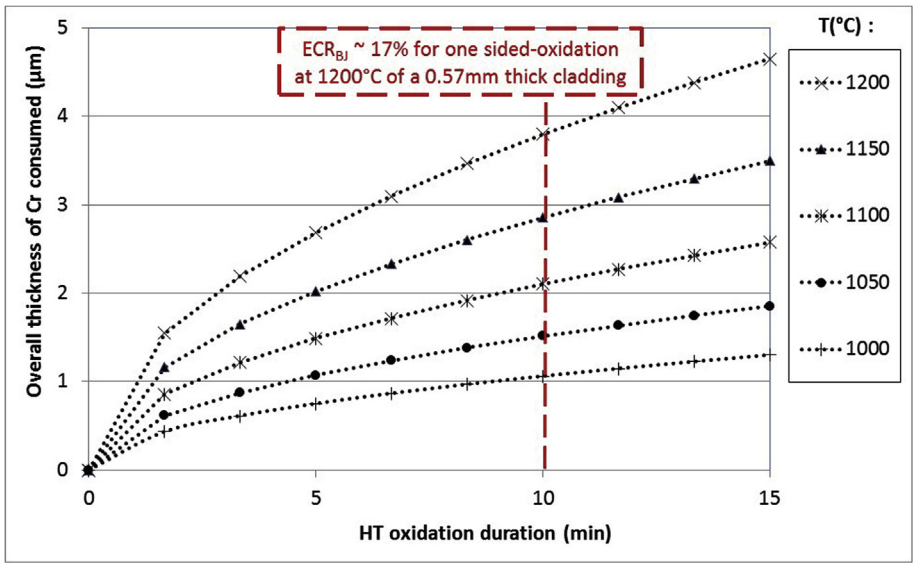


**Fig. 17.** Typical calculated Cr-coating overall consumption kinetics for DBA-LOCA oxidation times and temperatures 33.

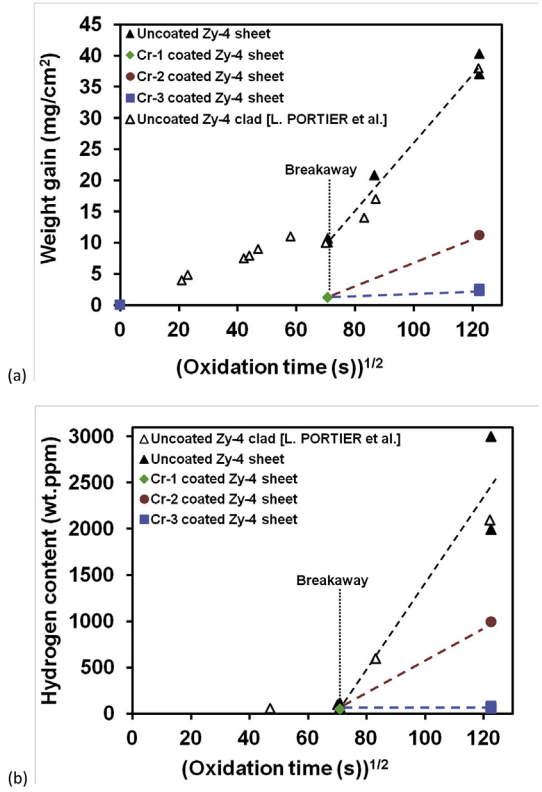


**Fig. 18.** Weight gain (a) and hydrogen up-take (b) of coated and uncoated (from L. PORTIER et al. [72]) Zircaloy-4 sheet samples, after steam oxidation up to 15000 s at 1000 °C 34.

with:

- D the Cr thermal (volume) diffusion coefficient in $\beta_{Zr}$ (from Ref. [94]), 6.29 $\mu m^2/s$ at 1200 °C,
- C(x, t) the Cr concentration diffusing into $\beta_{Zr}$ at a distance x from Zr-Cr interface, and for a given diffusion time t,
- $C_o$ the initial Cr concentration in the Zircaloy-4 substrate (~0.1 wt%),
- $C_s$ the concentration at the Cr/Zr interface assuming local thermodynamic equilibrium

Then the consumption kinetics of chromium at HT due to the inward chromium diffusion within the HT $\beta_{Zr}$ substrate can be calculated by integration of the Cr diffusion profiles. At 1200 °C, it is found that the Cr-coating consumption kinetics due to Cr diffusion into the substrate and due to outer chromia scale formation are nearly identical.

Finally, by summing the contributions of the outer oxidation (chromia scale formation) and the Cr diffusion into the substrate, and by using some additional experimental oxidation data obtained on Cr-coated Zircaloy-4 within the 1000–1300 °C temperature range, it was possible to derive a preliminary model of the overall Cr-coating consumption upon HT oxidation typical of DBA-LOCA conditions. It can be observed from Fig. 17 that, in agreement with the experimental results obtained, 5–10 µm thick Cr coating may survive to prototypical DBA-LOCA oxidation times and temperatures, that is, for ECR (calculated for the uncoated reference clad with the Baker-Just correlation) values and oxidation temperatures lower than 17% and 1200 °C respectively.

*HT steam oxidation of 5-12 µm Cr coated at 1000–1200°C for beyond DBA-LOCA oxidation times Zircaloy-4* – To have a first idea of the potential additional "coping period" which could be derived from the use of protective Cr-coatings before achieving full clad embrittlement due to HT oxidation, HT steam oxidation experiments were extended to longer oxidation times.

*Steam oxidation at 1000°C* – It is well known that for reference uncoated zirconium-based claddings, steam oxidation around 1000 °C is characterized by the occurrence of a "breakaway" oxidation phenomena after a certain "incubation" time, generally ranging from 3000 to 5000s for modern nuclear fuel alloys [95–102]. This phenomenon is characterized by an acceleration of the oxidation associated with a high hydrogen pick-up ratio. Fig. 18 shows the weight gain and hydrogen uptake of coated/uncoated Zircaloy-4 sheet samples after steam oxidation up to 15000 s at 1000 °C. It is obvious that for this post-breakaway oxidation time for the uncoated material, the uncoated materials have experienced severe oxidation with formation of thick outer zirconia scale with numerous cracks

**Table 2**
PQ mechanical properties obtained after HT steam oxidation at 1000 °C for 15000s followed by direct water quenching down to RT.

| Materials | Weight Gain ($mg/cm^2$) | Hydrogen content (wt.ppm) | Tensile test (sheet materials) | | | | Impact tests (clad segment) | RCT (clad segment) | |
|---|---|---|---|---|---|---|---|---|---|
| | | | YS ([a]) (MPa) | UTS ([a]) (MPa) | UE ([a]) (%) | TE ([a]) (%) | Impact energy ($J/mm^2$) | Max load (N) at RT *and at 135°C* | Residual ductility([b]) (%) at RT *and at 135°C* |
| Reference uncoated Zircaloy-4 | 37–40 | 2000 –3000 | – | 156 | – | 0 | Brittle/Failure upon quenching or upon PQ machining | | |
| 5–12 μm Cr coated Zircaloy-4 | 2.3–2.5 | ≤80 | 812 | 887 | 0.7 | 1.7 | 0.23 ([c]) | 1130-1270 *1560–1770* | 11.5–15 *>33* ([d]) |

[a] YS = Yield Strength at 0.2% plastic strain, UTS = Ultimate Tensile Strength, UE = Uniform Elongation, TE = Total Elongation (deduced from the crosshead displacement).
[b] Plastic displacement divided by the initial clad diameter (as defined in Ref. [75]).
[c] Embrittlement threshold ~0.04 $J/mm^2$ [71–73].
[d] No failure, until achievement of maximal displacement available on the RCT facility used.

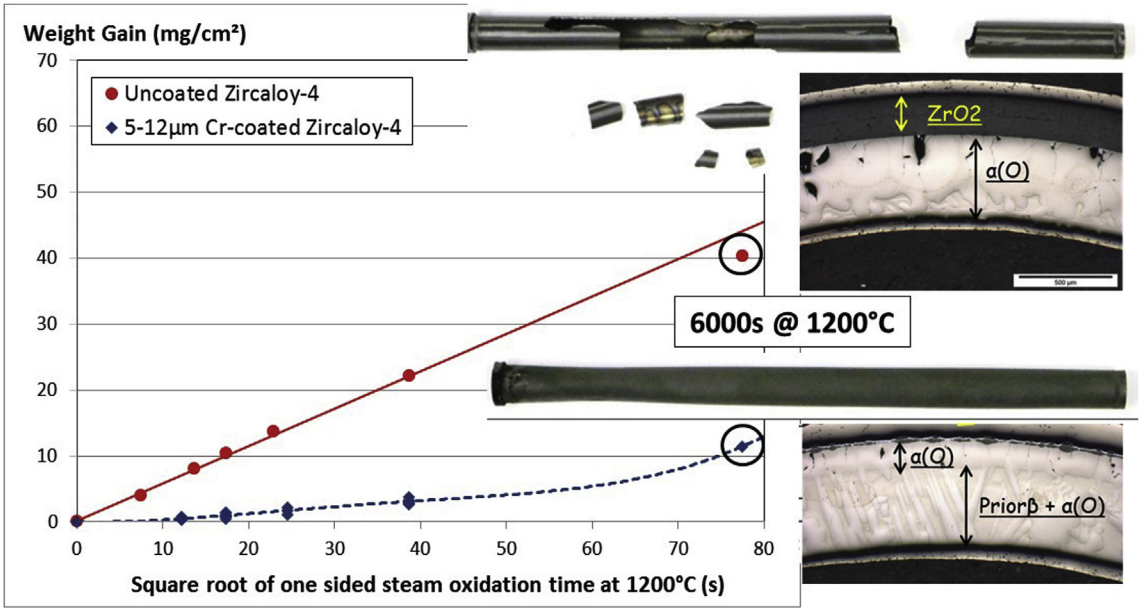


**Fig. 19.** Typical micrographs and weight gain evolution as a function the square root of (one-sided) oxidation time in steam at 1200 °C, for beyond DBA-LOCA oxidation times, for uncoated and 5–12 μm Cr-coated Zircaloy-4 sheet samples and clad segments 35.

and a very high hydrogen uptake. On the opposite and except for one particular not fully protective sample, Cr-coated Zircaloy-4 sheets are characterized by very low weight gain values corresponding to the formation of a 3-4 μm-thick outer chromia scale and negligible hydrogen uptake. PQ tensile tests, Ring Compression Tests (RCT) and impact tests (on samples with a U-shape notch) were carried out at RT. The results are summarized in Table 2. As discussed in more details in a previous paper [54], the PQ mechanical properties clearly show that for this beyond DBA-LOCA oxidation time, the Cr-coated Zircaloy-4 materials display high residual PQ strength, ductility and toughness while the uncoated Zircaloy-4 is fully brittle with very low or negligible residual strength and ductility. For this last one, its high brittleness is not only due to the formation of thick brittle $ZrO_2$ and $\alpha_{Zr}(O)$ layers but also to the high hydrogen and oxygen[8] concentrations within the residual inner prior-$\beta_{Zr}$ layer.

*Oxidation up to 6000 s at 1200°C*—6000 s at 1200 °C is nearly 10 times longer than the current LOCA criteria limit for one-sided oxidation of uncoated zirconium-based claddings at 1200 °C. It is obvious from Fig. 19 that, even if the outer Cr coating has been nearly fully consumed for such beyond DBA-LOCA conditions, the Cr-coated sample survived to the final quenching while the uncoated reference Zircaloy-4 clad segment did not. This confirms the capacity of the Cr-coated fuel cladding to sustain longer oxidation time at HT and/or higher temperature before loosing its integrity when compared to the reference uncoated materials.

*Impact of pre-existing (or formed upon clad ballooning) through-thickness cracks within the Cr coating on subsequent oxidation at HT* - As for in-service corrosion, the potential detrimental effect of damage of the Cr-coating on the subsequent HT steam oxidation behavior of the cladding is an important issue. Upon LOCA, such cracking of the Cr-coating may result from the internal pressure-induced clad ballooning as already observed and mentioned in the previous chapter for ceramic-based coatings (CrN). As an illustration, Fig. 20 shows a typical SEM fractograph of a first generation (not fully protective) Cr-coated Zircaloy-4 sheet sample that has been subjected to steam oxidation for 300 s at 1200 °C followed by direct water quenching, and then tensile-tested at RT. As already observed and discussed in Ref. [106] for multilayered TiN-TiAlN

[8] The high oxygen concentration achieved of nearly 0,9 wt.% is much higher than the equilibrium oxygen solubility in the $\beta_{Zr}$ phase of as-received uncoated Zircaloy-4 (~0,25 wt.% at 1000°C). As discussed in Ref. [54] and consistently with thermodynamic predictions, this is related to the thermodynamic "β-stabilizing" effect of hydrogen which increases the $\beta_{Zr}$ oxygen solubility [103–105].

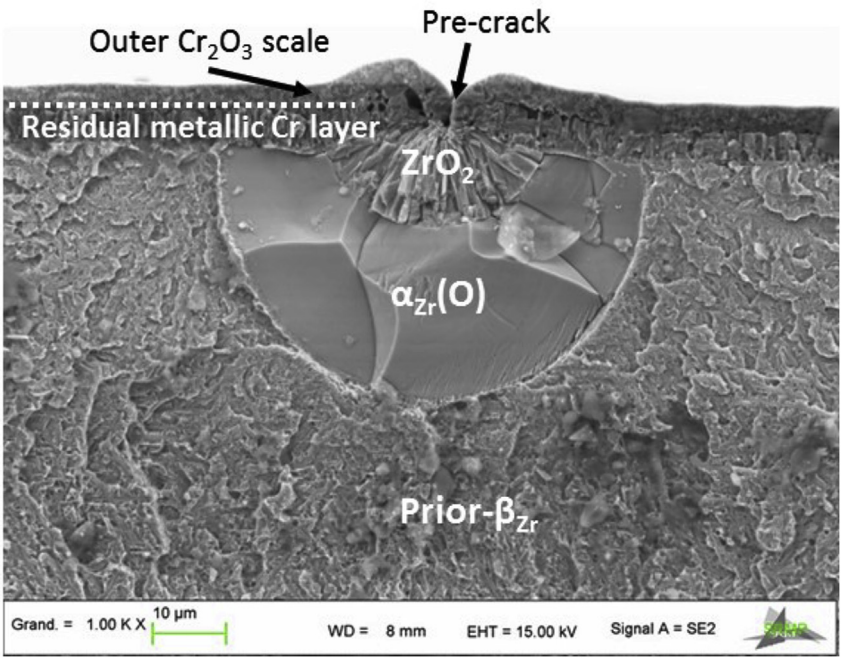


**Fig. 20.** SEM fractograph of (not fully protective) Cr-coated Zircaloy-4 sheet sample from a first generation that has been subjected to steam oxidation for 300 s at 1200 °C followed by direct water quenching, and then tensile-tested at RT 35.

coating system over Zirlo™ substrate exposed to supercritical water, it can be observed that the pre-existing crack within the Cr-coating induced some localized oxidation of the Zircaloy-4 substrate at HT, with formation of a ~10 µm-thick nodular zirconia "spot" and a ~20 µm-thick $\alpha_{Zr}(O)$ "ring" just underneath. Let us remind that for the reference uncoated Zircaloy-4 sheet sample tested in the same conditions, 50-60 µm-thick oxide and $\alpha_{Zr}(O)$ layers formed. Then, taking into account the perfect spherical shape of the oxygen penetration depth beneath the pre-existing crack in Cr, it can be concluded that this type of pre-existing defect does not induce any local acceleration of the subsequent HT oxidation of the substrate. Additionally, the aspect of Cr suggests that the formation of an outer chromia scale at the crack "lips" tends to close the pre-existing defect due to the ($Cr_2O_3$) volume expansion induced locally inside the crack, thus further reducing the access of steam to the Zircaloy-4 substrate (*i.e.*, partial "self-healing" effect). This last assumption should explain the thinner zirconia and $\alpha_{Zr}(O)$ formed within the Cr-coated Zircaloy-4 substrate as an extension of the Cr crack-tip, when compared to the deeper oxidation observed for the uncoated reference materials. Finally, it can be observed that in the vicinity of the nodular $ZrO_2$ oxide spot, where local swelling has occurred, the outer chromium oxide and the remaining metallic layers were still remarkably fully adherent to the Zircaloy-4 substrate. This indicates that such a defect should not induce extended spalling of the Cr coating upon HT oxidation or during the final water quenching.

## 4. Conclusions

Coatings with thicknesses between a few microns and ~10 µm deposited on a Zircaloy-4 substrate were studied with the objective to provide a significant reduction in the oxidation-induced embrittlement of the nuclear fuel cladding, especially in accidental conditions, such as LOCA conditions. Early studies were performed at CEA on several types of coatings fabricated by a PVD process, including ceramic nitride and metallic multi-layered coatings. The results of this screening analysis showed that the first generation of chromium-based coatings exhibited the most promising behavior with a good compromise between nominal corrosion resistance and adhesion of the coating, good fretting resistance and improved resistance to steam oxidation at HT, relevant of DBA-LOCA conditions and slightly beyond.

These preliminary encouraging results were further confirmed on the last generation of Cr-coated M5™ as discussed in some other papers [54–63].

## Acknowledgments

Numerous people took part of this study at CEA and the authors want to thank them all.

Special thanks to: P. Wident for having carried out some of the mechanical tests, P. Billaud and C. Hossepied for having performed the autoclave tests and some of the hydrogen measurements, H. Palancher, P. Bossis, L. Portier, A. Soniak and T. Forgeron for their advising and organizing support.

This study has been partially conducted under the french nuclear institute partnership between Framatome, EDF and CEA. Specific thanks to Jérémy Bischoff and Christine Delafoy from Framatome and Edouard Pouillier, Nicolas Waeckel and Marie Moatti from EDF.

## Appendix A. Supplementary data

Supplementary data to this article can be found online at https://doi.org/10.1016/j.jnucmat.2019.02.018.

## References

[1] J. Carmack, F. Goldner, S.M. Bragg-Sitton, L.L. Snead, Overview of the US DOE Accident Tolerant Fuel Development Program, Idaho National Laboratory (INL), 2013.
[2] S.J. Zinkle, K.A. Terrani, J.C. Gehin, L.J. Ott, L.L. Snead, Accident tolerant fuels for LWRs: a perspective, J. Nucl. Mater. 448 (2014) 374–379.
[3] S. Bragg-Sitton, Development of advanced accident-tolerant fuels for

commercial LWRs, Nucl. News 53 (2014) 83–91.
[4] Y.-H. Koo, J.-H. Yang, J.-Y. Park, K.-S. Kim, H.-G. Kim, D.-J. Kim, et al., KAERI's development of LWR accident tolerant fuel, Nucl. Technol. 186 (2014), 295–30.
[5] J.C. Brachet, C. Lorrette, A. Michaux, C. Sauder, I. Idarraga-Trujillo, M. Le Saux, M. Le Flem, F. Schuster, A. Billard, E. Monsifrot, E. Torres, F. Rebillat, J. Bischoff, A. Ambard, CEA studies on advanced nuclear fuel claddings for enhanced accident tolerant LWRs fuel (LOCA and beyond LOCA conditions), in: Fontevraud 8: Conference on Contribution of Materials Investigations and Operating Experience to LWRs' Safety, Performance and Reliability; Avignon (France), 15-18 Sep 2014.
[6] M. Kurata, Research and development methodology for practical use of accident tolerant fuel in light water reactors, Nucl. Eng. Technol. 48 (2016) 26–32.
[7] J. Bischoff, K. McCoy, J. Strumpell, J.-C. Brachet, C. Lorrette, Development of fuels with enhanced accident tolerance, in: Proceedings of TopFuel Conference 2015, Zurich, Switzerland, Sept. 2015.
[8] Z. Duan, H. Yang, Y. Satoh, K. Murakami, S. Kano, Z. Zhao, J. Shen, H. Abe, Current status of materials development of nuclear fuel cladding tubes, for light water reactors, Nucl. Eng. Des. 316 (2017) 131–150.
[9] K.A. Terrani, Accident tolerant fuel cladding development: promise, status, and challenges, J. Nucl. Mater. 501 (2018), https://doi.org/10.1016/j.jnucmat.2017.12.043.
[10] H. Palancher et al., "Advances in ATF R&D at CEA", Proceedings of "Fuel Reliability Program Winter Technical Advisory Committee Meeting, 7th. EPRI/INL/DOE Joint Workshop on Accident Tolerant Fuel", (21-22 February 2018), Ft. Worth, USA.
[11] K.A. Terrani, C.M. Parish, D. Shin, B.A. Pint, Protection of zirconium by alumina- and chromia-forming iron alloys under high-temperature steam exposure, J. Nucl. Mater. (2013) 64–71, https://doi.org/10.1016/j.jnucmat.2013.03.006.
[12] J.Y. Park, I.H. Kim, Y.I. Jung, H.G. Kim, D.J. Park, B.K. Choi, High temperature steam oxidation of Al3Ti-based alloys for the oxidation-resistant surface layer on Zr fuel claddings, J. Nucl. Mater. 437 (2013) 75–80.
[13] F. Khatkhatay, L. Jiao, J. Jian, W. Zhang, Z. Jiao, J. Gan, H. Zhang, X. Zhang, H. Wang, Superior corrosion resistance properties of TiN-based coatings on Zircaloy tubes in supercritical water, J. Nucl. Mater. 451 (2014) 346–351.
[14] H.-G. Kim, I.-H. Kim, Y.-I. Jung, D.-J. Park, J.-Y. Park, Y.-H. Koo, Adhesion property and high-temperature oxidation behavior of Cr-coated Zircaloy-4 cladding tube prepared by 3D laser coating, J. Nucl. Mater. 465 (2015) 531–539.
[15] K. Daub, R. Van Nieuwenhove, H. Nordin, Investigation of the impact of coatings on corrosion and hydrogen uptake of Zircaloy-4, J. Nucl. Mater. 467 (2015) 260–270.
[16] A.S. Kuprin, V.A. Belous, V.N. Voyevodin, V.V. Bryk, R.L. Vasilenko, V.D. Ovcharenko, et al., Vacuum-arc chromium-based coatings for protection of zirconium alloys from the high-temperature oxidation in air, J. Nucl. Mater. 465 (2015) 400–406, https://doi.org/10.1016/J.JNUCMAT.2015.06.016.
[17] J.H. Park, H.-G. Kim, J. Park, Y.-I. Jung, D.-J. Park, Y.-H. Koo, High temperature steam-oxidation behavior of arc ion plated Cr coatings for accident tolerant fuel claddings, Surf. Coating. Technol. 280 (2015) 256–259.
[18] E. Alat, A.T. Motta, R.J. Comstock, J.M. Partezana, D.E. Wolfe, Ceramic coating for corrosion (c3) resistance of nuclear fuel cladding, Surf. Coating. Technol. 281 (2015) 133–143.
[19] B.R. Maier, B.L. Garcia-Diaz, B. Hauch, L.C. Olson, R.L. Sindelar, K. Sridharan, Cold spray deposition of Ti2AlC coatings for improved nuclear fuel cladding, J. Nucl. Mater. 466 (2015) 712–717, https://doi.org/10.1016/J.JNUCMAT.2015.06.028.
[20] E. Alat, A.T. Motta, R.J. Comstock, J.M. Partezana, D.E. Wolfe, Multilayer (TiN, TiAlN) ceramic coatings for nuclear fuel cladding, J. Nucl. Mater. 478 (2016) 236–244.
[21] D.J. Park, H.G. Kim, Y. Il Jung, J.H. Park, J.H. Yang, Y.H. Koo, Behavior of an improved Zr fuel cladding with oxidation resistant coating under loss-of-coolant accident conditions, J. Nucl. Mater. 482 (2016) 75–82.
[22] H. Yeom, B. Hauch, G. Cao, B. Garcia-Diaz, M. Martinez-Rodriguez, H. Colon-Mercado, et al., Laser surface annealing and characterization of Ti 2 AlC plasma vapor deposition coating on zirconium-alloy substrate, Thin Solid Films 615 (2016) 202–209.
[23] I. Younker, M. Fratoni, Neutronic evaluation of coating and cladding materials for accident tolerant fuels, Prog. Nucl. Energy 88 (2016) 10–18, https://doi.org/10.1016/j.pnucene.2015.11.006.
[24] J. Carr, G. Vasudevamurthy, L. Snead, B. Hinderliter, C. Massey, Investigations of aluminum-doped self-healing zircaloy surfaces in context of accident-tolerant fuel cladding Research, J. Mater. Eng. Perform. 25 (6) (June 2016) 2347–2355.
[25] H. Yeom, B. Maier, R. Mariani, D. Bai, K. Sridharan, Evolution of multilayered scale structures during high temperature oxidation of ZrSi2, J. Mater. Res. 31 (21) (Nov 14, 2016).
[26] D. Jin, F. Yang, Z. Zou, L. Gu, X. Zhao, F. Guo, P. Xiao, A study of the zirconium alloy protection by Cr3C2–NiCr coating for nuclear reactor application, Surf. Coating. Technol. 287 (2016) 55–60.
[27] W. Zhong, P.A. Mouche, X. Han, B.J. Heuser, K.K. Mandapaka, G.S. Was, Performance of iron-chromium-aluminum alloy surface coatings on Zircaloy 2 under high-temperature steam and normal BWR operating conditions, J. Nucl. Mater. 470 (2016) 327–338.
[28] V.M. Borisov, V.N. Trofimov, A.Y. Sapozhkov, V.A. Kuzmenko, V.B. Mikhaylov, V.Y. Cherkovets, A.A. Yakushkin, V.L. Yakushin, P.S. Dzhumayev, "Capabilities to improve corrosion resistance of fuel claddings by using powerful laser and plasma sources", ISSN 1063-7788, Phys. Atom. Nucl. 79 (14) (2016) 1656–1662.
[29] Y. Lee, J.I. Lee, H.C. No, Mechanical analysis of surface-coated zircaloy cladding, Nucl. Eng. Technol. 49 (2017) 1031–1043.
[30] H. Shah, J. Romero, P. Xu, B. Maier, G. Johnson, J. Walters, et al., Development of surface coatings for enhanced accident tolerant fuel, in: Water React. Fuel Perform. Meet., Jeju Island, Korea, 2017.
[31] H.-G. Kim, I.-H. Kim, Y.-I. Jung, D.-J. Park, J.-H. Park, J.-H. Yang, et al., Progress of surface modified Zr cladding development for ATF at KAERI, in: Water React. Fuel Perform. Meet., Jeju Island, Korea, 2017.
[32] R. Van Nieuwenhove, V. Andersson, J. Balak, B. Oberländer, In-pile testing of CrN, TiAlN and AlCrN coatings on zircaloy cladding in the halden reactor, in: 18th Int. Symp. Zircon. Nucl. Ind. STP1597, Hilton Head, SC, 2017.
[33] M.J. Brova, E. Alat, M.A. Pauley, R. Sherbondy, A.T. Motta, D.E. Wolfe, Undoped and ytterbium-doped titanium aluminum nitride coatings for improved oxidation behavior of nuclear fuel cladding, Surf. Coating. Technol. (2017).
[34] J. Skarohlid, R. Skoda, High temperature behaviour of CrAlSiN max phase coatings on zirconium alloy, in: Water React. Fuel Perform. Meet., Jeju Island, Korea, 2017.
[35] C. Tang, M. Stueber, H.J. Seifert, M. Steinbrueck, Protective coatings on zirconium-based alloys as accident tolerant fuel (ATF) claddings, Corros. Rev. 35 (2017) 141–165.
[36] C. Tang, M. Steinbrueck, M. Stueber, M. Grosse, X. Yub, S. Ulrich, H.J. Seifert, Deposition, characterization and high-temperature steam oxidation behavior of single-phase Ti2AlC-coated Zircaloy-4, Corros. Sci. 135 (2018) 87–98.
[37] Z. Gao, Y. Chen, J. Kulczyk-Malecka, P. Kelly, Y. Zeng, X. Zhang, C. Li, H. Liu, N. Rohbeck, P. Xiao, Comparison of the Oxidation Behavior of a Zirconium Nitride Coating in Water Vapor and Air at High Temperature, Corrosion Science, 2018. https://doi.org/10.1016/j.corsci.2018.04.015.
[38] C. Tang, M. Steinbrueck, M. Grosse, S. Ulrich, M. Stueber, H.J. Seifert, Improvement of the high-temperature oxidation resistance of Zr alloy cladding by surface modification with aluminium-containing ternary carbides, in: Proceedings of ICAPP 2018, Charlotte, North Carolina, USA, April 8-11, 2018.
[39] D.J. Park, H.G. Kim, Y.I. Jung, J.H. Park, J.H. Yang, Y.H. Koo, Microstructure and mechanical behavior of Zr substrates coated with FeCrAl and Mo by cold-spraying, J. Nucl. Mater. 504 (2018) 261–266.
[40] D. Jin, N. Ni, Y. Guo, Z. Zou, X. Wang, F. Guo, X. Zhao, P. Xiao, Corrosion of the bonding at FeCrAl/Zr alloy interfaces in steam, J. Nucl. Mater. 508 (2018) 411–422.
[41] D. Park, P.A. Mouche, W. Zhong, K.K. Mandapaka, G.S. Was, B.J. Heuser, TEM/STEM study of Zircaloy-2 with protective FeAl(Cr) layers under simulated BWR environment and high-temperature steam exposure, J. Nucl. Mater. 502 (2018) 95–105.
[42] H. Yeom, B. Maier, G. Johnson, T. Dabney, J. Walters, K. Sridharan, Development of cold spray process for oxidation-resistant FeCrAl and Mo diffusion barrier coatings on optimized ZIRLO™, J. Nucl. Mater. 507 (2018) 306–315.
[43] H. Yeom, C. Lockhart, R. Mariani, P. Xu, M. Corradini, K. Sridharan, Evaluation of steam corrosion and water quenching behavior of zirconium-silicide coated LWR fuel claddings, J. Nucl. Mater. 499 (2018) 256–267.
[44] W. Zhong, P.A. Mouche, B.J. Heuser, Response of Cr and Cr-Al coatings on Zircaloy-2 to high temperature steam, J. Nucl. Mater. 498 (2018) 137–148.
[45] M. Sevecek, A. Gurgen, A. Seshadri, Y. Che, M. Wagih, B. Phillips, V. Champagne, K. Shirvan, Development of Cr cold spray-coated fuel cladding with enhanced accident tolerance, Nucl. Eng. Tech. (2018). https://doi.org/10.1016/j.net.2017.12.011.
[46] A. Gurgen, K. Shirvan, Estimation of coping time in pressurized water reactors for near term accident tolerant fuel claddings, Nucl. Eng. Des. 337 (2018) 38–50.
[47] Y. Dong, F. Ge, F. Meng, G. Zhao, J. Zhou, Z. Deng, Q. Huang, F. Huang, Improved oxidation resistance of zirconium at high-temperature steam by magnetron sputtered Cr-Al-Si ternary coatings, Surf. Coating. Technol. (2018). https://doi.org/10.1016/j.surfcoat.2018.04.029.
[48] Y. Wang, W. Zhou, Q. Wen, X. Ruan, F. Luo, G. Bai, Y. Qing, D. Zhu, Z. Huang, Y. Zhang, T. Liu, R. Li, Behavior of plasma sprayed Cr coatings and FeCrAl coatings on Zr fuel cladding under loss-of-coolant accident conditions, Surf. Coating. Technol. 344 (2018) 141–148.
[49] W. Zhang, R. Tang, Z.B. Yang, C.H. Liu, H. Chang, J.J. Yang, J.L. Liao, Y.Y. Yang, N. Liu, Preparation, structure, and properties of an AlCrMoNbZr high-entropy alloy coating for accident-tolerant fuel cladding, Surf. Coating. Technol. 347 (2018) 13–19.
[50] Y. Wang, H. Tang, X. Han, W. Feng, X. Zhou, S. Peng, H. Zhang, Oxidation resistance improvement of Zr-4 alloy in 1000°C steam environment using ZrO2/FeCrAl bilayer coating, Surf. Coating. Technol. (2018), https://doi.org/10.1016/j.surfcoat.2018.05.005.
[51] D. Jin, Y. Guo, Z. Gao, Y. Zhou, X. Wang, F. Guo, X. Zhao, P. Xiao, Investigation on the oxidation and corrosion behaviors of FeCrZr alloy as a protective material for Zr cladding, J. Alloy. Comp. (2018), https://doi.org/10.1016/j.jallcom.2018.04.250P.
[52] P. Baque, R. Darras, A. Lafon, H. Loriers, Protection du zirconium contre

l'oxydation au moyen de revêtements métalliques (Protection of zirconium and its alloys by metallic coatings), J. Nucl. Mater. 25 (1968) 166–171 (– in french).
[53] H. Loriers, A. Lafon, R. Darras, P. Baque, Protection of Zirconium and its Alloys by Metallic Coatings, CEA Report CEA-R-3612, 1968 (- in french).
[54] I. Idarraga-trujillo, M. Le Flem, J.-C. Brachet, M. Le Saux, D. Hamon, S. Muller, V. Vandenberghe, M. Tupin, E. Papin, A. Billard, E. Monsifrot, F. Schuster, Assessment at CEA of coated nuclear fuel cladding for LWRs with increased margins in LOCA and beyond LOCA conditions, in: Proceedings of 2013 LWR Fuel Performance Meeting/TopFuel, Charlotte, NC, USA, Sept. 15-19, 2013.
[55] J.C. Brachet, M. Le Saux, M. Le Flem, S. Urvoy, E. Rouesne, T. Guilbert, C. Cobac, F. Lahogue, J. Rousselot, M. Tupin, P. Billaud, C. Hossepied, F. Schuster, F. Lomello, A. Billard, G. Velisa, E. Monsifrot, J. Bischoff, A. Ambard, On-going studies ar CEA on chromium coated zirconium based nuclear fuel claddings for enhanced accident tolerant LWR fuel, in: Proceedings of TopFuel Conference 2015, Zurich, Switzerland, September 2015.
[56] J.C. Brachet, M. Le Saux, V. Lezaud-Chaillioux, M. Dumerval, Q. Houmaire, F. Lomello, F. Schuster, E. Monsifrot, J. Bischoff, E. Pouillier, Behavior under LOCA conditions of enhanced accident tolerant chromium coated zircaloy-4 claddings, in: Proceedings of TopFuel 2016 Conference, Boise, ID, USA, September 2016.
[57] J. Bischoff, C. Delafoy, P. Barberis, D. Perche, B. Buerin, J.-C. Brachet, Development of Cr-coated zirconium cladding for enhanced accident tolerance, in: Proceedings of TopFuel Conference 2016, Boise, ID, USA, September 2016.
[58] J. Bischoff, C. Delafoy, C. Vauglin, P. Barberis, C. Roubeyrie, D. Perche, D. Duthoo, F. Schuster, J.-C. Brachet, E.W. Schweitzer, K. Nimishakavi, AREVA NP's enhanced accident tolerant fuel developments: focus on Cr-coated M5 cladding, Nucl. Eng. Tech. 50 (2018) 223–228.
[59] J.C. Brachet, M. Dumerval, V. Lezaud-Chaillioux, M. Le Saux, E. Rouesne, D. Hamon, S. Urvoy, T. Guilbert, Q. Houmaire, C. Cobac, G. Nony, J. Rousselot, F. Lomello, F. Schuster, H. Palancher, J. Bischoff, E. Pouillier, Behavior of chromium coated M5 claddings under LOCA conditions, in: Proceedings of WRFPM Conference, Jeju, Republic of South Korea, September 2017.
[60] C. Delafoy, J. Bischoff, J. Larocque, P. Attal, L. Gerken, K. Nimishakavi, Benefits of Framatome's E-ATF evolutionary solution: Cr-coated cladding with Cr2O3-doped UO2 fuel, in: Proceedings of TopFuel 2018, Prague, Czech Republic, September 2018.
[61] J.C. Brachet, T. Guilbert, M. Le Saux, J. Rousselot, G. Nony, C. Toffolon-Masclet, A. Michau, F. Schuster, H. Palancher, J. Bischoff, J. Augereau, E. Pouillier, « Behavior of Cr-coated M5 claddings during and after high temperature steam oxidation from 800°C up to 1500°C (LOss-of-Coolant Accident & Design Extension Conditions)", Proceedings of WRFPM/TOPFUEL 2018, (30 Sept. – 04 Oct. 2018), Prague, Czech Republic.
[62] M. Dumerval, Q. Houmaire, J.C. Brachet, H. Palancher J. Bischoff, E. Pouillier, « behavior of chromium coated M5 claddings upon thermal ramp tests under internal pressure (LOss-of-Coolant accident conditions)", Proceedings of WRFPM/TOPFUEL 2018, (30 Sept. – 04 Oct. 2018), Prague, Czech Republic.
[63] J. Bischoff, C. Delafoy, N. Chaari, C. Vauglin, K. Buchanan, P. Barberis, F. Schuster, J-C Brachet, K. Nimishakavi, "Cr-coated cladding development at Framatome", Proceedings of WRFPM/TOPFUEL 2018, (30 Sept. – 04 Oct. 2018), Prague, Czech Republic.
[65] J.A. Thornton, D.W. Hoffman, Stress-related effects in thin films, Thin Solid Films 171 (1989) 5–31.
[66] W. Xiao, H. Deng, S. Zou, Y. Ren, D. Tang, M. Lei, C. Xiao, X. Zhou, Y. Chen, « Effect of roughness of substrate and sputtering power on the propertis of TiN coatings deposited by magnetron sputtering for ATF », J. Nucl. Mater. 509 (2018) 542–549.
[67] J. Ribis, A. Wu, J.C. Brachet, F. Barcelo, B. Arnal, Atomic-scale interface structure of a Cr-coated Zircaloy-4 material, J. Mat. Sci. (2018).
[68] A. Wu, J. Ribis, J.C. Brachet, E. Clouet, F. Leprêtre, E. Bordas, B. Arnal, HRTEM and chemical study of an ion-irradiated chromium/zircaloy-4 Interface, J. Nucl. Mater. 504 (2018) 289–299.
[69] I.C. Noyan, J.B. Cohen (Eds.), Residual Stress, Measurement by Diffraction and Interpretation, Springer, 1986.
[70] A. Wu, Study of the Behavior before and after Ion Irradiation of Chromium Coated Zirconium Alloy for Use as an Innovative Nuclear Fuel Cladding in LWRs, PhD thesis manuscript, Pierre et Marie Curie University, 2017 (– in French).
[71] J.C. Brachet et al., "Mechanical behavior at room temperature and metallurgical study of low-tin Zy-4 and M5™ alloys after oxidation at 1100°C and quenching", Proceedings of the Technical Committee Meeting on Fuel Behavior under Transient and LOCA Conditions, IAEA-TECDOC-1320, Halden, Norway, (Sept 10–14, 2001), pp. 139-158.
[72] L. Portier, T. Bredel, J.C. Brachet, V. Maillot, J.P. Mardon, A. Lesbros, "Influence of long service exposures on the thermal-mechanical behaviour of Zy-4 and M5™ alloys in LOCA conditions", J. ASTM Int. (JAI) 2 (2005) JAI12468.
[73] J.C. Brachet, V. Maillot, L. Portier, D. Gilbon, A. Lesbros, N. Waeckel, J.P. Mardon, Hydrogen content, pre oxidation and cooling scenario influences on post-quench mechanical properties of Zy-4 and M5™ alloys in LOCA conditions - relationship with the post-quench microstructure, J. ASTM Int. (JAI) 5 (4) (2008). Paper ID JAI101116.
[74] M. Le Saux, et al., Influence of pre-transient oxide on LOCA high temperature steam oxidation and post-quench mechanical properties of zircaloy-4 and M5™ cladding, in: Water Reactor Fuel Performance (Topfuel) Meeting, Chengdu, China, (Sept. 11-14, 2011), Paper T3-040M, 2011.
[75] Y. Yan Billone, T. Burtseva, R. Daum, Cladding Embrittlement during Postulated Loss-Of-Coolant Accidents, NUREG/CR-6967/ANL-07/04 Report, June 30, 2008.
[76] F. Nagase, T. Fuketa, Effect of pre-hydriding on thermal shock resistance of zircaloy-4 cladding under simulated loss-of-coolant accident conditions, J. Nucl. Sci. Technol. 41 (7) (2004) 723–730.
[77] F. Nagase, T. Chuto, T. Fuketa, Behavior of high burn-up fuel cladding under LOCA conditions, J. Nucl. Sci. Technol. 46 (7) (2009) 763–769.
[78] J.C. Brachet, D. Hamon, J.L. Béchade, P. Forget, C. Toffolon-Masclet, C. Raepsaet, J.P. Mardon, B. Sebbari, Quantification of the Chemical Elements Partitioning within Pre-hydrided Zircaloy-4 after High Temperature Steam Oxidation as a Function of the Final Cooling Scenario (LOCA Conditions) and Consequences on the (Local) Materials Hardening, IAEA-TECDOC-CD-1709, 2013, pp. 253–265.
[79] A. Sawatzki, G.A. Ledoux, S. Jones, Oxidation of zirconium during a high temperature transient, in: A.L. Lowe Jr., G.W. Parry (Eds.), Zirconium in the Nuclear Industry, ASTM STP 633, American Society for Testing materials, 1977, pp. 134–149.
[80] H.M. Chung, T.F. Kassner, Embrittlement Criteria for Zircaloy Fuel Cladding Applicable to Accident Situations in Light-Water Reactors, Summary Report, NUREG/CR-1344, ANL-7948, 1980.
[81] M. Négyesi, L. Novotný, J. Kabátová, S. Linhart, V. Klouček, J. Lorinčík, V. Vrtílková, UJP LOCA Oxidation Criteria "K" and "Oβ", IAEA-TECDOC-CD-1709, 2013.
[82] A. Michau, F. Maury, F. Schuster, F. Lomello, J.C. Brachet, E. Rouesne, M. Le Saux, R. Boichot, M. Pons, High-temperature Oxidation Resistance of Chromium-Based Coatings Deposited by DLI-MOCVD Process for Enhanced Protection of the Inner Surface of Long Tubes, Surface & Coatings Technology, 2018, https://doi.org/10.1016/J.SURFCOAT.2018.05.088.
[84] A. Aubert, R. Gillet, A. Gaucher, J.P. Terrat, Hard chrome coatings deposited by physical vapour deposition, Thin Solid Films 108 (1983) 165–172.
[85] G. Cholvy, J.L. Derep, M. Gantois, Characterization and wear resistance of coatings in the Cr-C-N ternary system deposited by physical vapour deposition, Thin Solid Films 126 (1985) 51–60.
[86] F. Cosset, G. Contoux, A. Celerier, J. Machet, Deposition of corrosion-resistant chromium and nitrogen-doped chromium coatings by cathodic magnetron sputtering, Surf. Coating. Technol. 79 (1996) 25–34.
[87] C. Gautier, J. Machet, Effects of deposition parameters on the texture of chromium films deposited by vacuum arc evaporation, Thin Solid Films 289 (1996) 34–38.
[88] J. Pina, A. Dias, M. Francois, J.L. Lebrun, Residual stresses and crystallographic texture in hard-chromium electroplated coatings, Surf. Coating. Technol. 96 (1997) 148–162.
[89] U. Holzwarth, H. Stamm, Mechanical and thermomechanical properties of commercially pure chromium and chromium alloys, J. Nucl. Mater. 300 (2002) 161–177.
[90] Y.F. Gu, H. Harada, Y. Ro, Chromium and chromium-based alloys: problems and possibilities for high-temperature service, JOM (Sept. 2004) 28–32.
[92] N. Dupin, I. Ansara, C. Servant, C. Toffolon, C. Lemaignan, J.C. Brachet, A thermodynamic database for zirconium alloys, J. Nucl. Mater. 275 (1999) 287–295.
[93] P. Lafaye, PhD Thesis, Paris-Est University (2017) (- in French).
[94] Landolt-börnstein book, in: H. Mehrer (Ed.), Diffusion in Solid Metals and Alloys, vol. 26, 1990.
[95] S. Leistikow, G. Schanz, Oxidation kinetics and related phenomena of zircaloy-4 fuel cladding exposed to high temperature steam and hydrogen-steam mixtures under PWR accident conditions, Nucl. Eng. Des. 103 (1987) 65–84.
[96] M. Billone, Y. Yan, T. Burtseva, R. Daum, Cladding Embrittlement during Postulated Loss-Of-Coolant Accidents, NUREG/CR-6967, Argonne National Laboratory, Lemont, IL, 2008.
[97] J.H. Baek, Y.H. Jeong, Breakaway phenomenon of Zr-based alloys during a high-temperature oxidation, J. Nucl. Mater. 372 (2008) 152–159.
[98] F. Nagase, T. Otomo, H. Uetsuka, Oxidation kinetics of low-Sn zircaloy-4 at the temperature range from 773 to 1573K, J. Nucl. Sci. Technol. 40 (2003) 213–219.
[99] V. Vandenberghe, J.C. Brachet, M. Le Saux, D. Gilbon, J.P. Mardon, B. Sebbari, Sensitivity to chemical composition variations and heating/oxidation mode of the breakaway oxidation in M5® cladding steam oxidized at 1000°C (LOCA conditions), in: Proceedings of TopFuel 2012, Manchester, UK, September 2-6, 2012.
[100] Z. Hózer, C. Gyori, L. Matus, M. Horváth, Ductile-to-brittle transition of oxidised Zircaloy-4 and E110 claddings, J. Nucl. Mater. 373 (2008) 415–423.
[101] D.J. Park, J.Y. Park, Y.H. Jeong, J.Y. Lee, Microstructural characterization of $ZrO_2$ layers formed during the transition to breakaway oxidation, J. Nucl. Mater. 399 (2010) 208–211.
[102] M. Steinbrück, J. Birchley, A.V. Boldyrev, A.V. Goryachev, M. Große, T.J. Haste, Z. Hózer, A.E. Kisselev, V.I. Nalivaev, V.P. Semishkin, L. Sepold, J. Stuckert, N. Vér, M.S. Veshchunov, High-temperature oxidation and quench behaviour of Zircaloy-4 and E110 cladding alloys, Prog. Nucl. Energy 52 (2010) 19–36.
[103] J.C. Brachet, L. Portier, T. Forgeron, J. Hivroz, D. Hamon, T. Guilbert, T. Bredel, P. Yvon, J.P. Mardon, P. Jacques, ASTM STP 1423, in: G.D. Moan, P. Rudling (Eds.), Influence of Hydrogen Content on the α↔β Phase Transformation Temperatures and on the Thermal-Mechanical Behavior of Zy-4, M4

(ZrSnFeV) and M5™ (ZrNbO) Alloys during the First Phase of LOCA Transient, American Society for Testing and Materials, West Conshohocken, PA, 2002, pp. 673–701.
[104] B. Mazères, C. Desgranges, C. Toffolon-Masclet, D. Monceau, Contribution to modeling of hydrogen effect on oxygen diffusion in Zy-4 alloy during high temperature steam oxidation, Oxid. Met. 79 (2013) 121–133.
[105] J.C. Brachet, D. Hamon, M. Le Saux, V. Vandenberghe, C. Toffolon-Masclet, E. Rouesne, S. Urvoy, J.L. Béchade, C. Raepsaet, J.L. Lacour, G. Bayon, F. Ott, Study of secondary hydriding at high temperature in zirconium based nuclear fuel cladding tubes by coupling information from neutron radiography/tomography, electron probe micro analysis, micro elastic recoil detection analysis and laser induced breakdown spectroscopy microprobe, J. Nucl. Mater. 488 (2017) 267–286.
[106] K.K. Mandapaka, R.S. Cahyadi, S. Yalisove, W. Kuang, K. Sickafus, M.K. Patel, G.S. Was, Corrosion behavior of ceramic-coated ZIRLO™exposed to supercritical water, J. Nucl. Mater. 498 (2018) 495–504.